Ghent University &
Max Planck Institute for Marine Microbiology

Faculty of Sciences

Marine Biology Research Group &
Helmholtz - Max Planck Joint Research Group
for Deep-Sea Ecology and Technology

Academic Year 2014-2015

The relation between biodiversity and biogeochemical functioning in Arctic deep sea sediments

Naomi De Roeck

Dr. Ulrike Braeckman

Dr. Ellen Pape

Liesbet Colson

Master thesis submitted for the partial fulfilment of the title of

Master of Science in Marine Biodiversity and Conservation

within the International Master of Science in Marine Biodiversity and Conservation
EMBC+

‘No data can be taken out of this work without prior approval of the thesis-promoter'

I hereby confirm that I have independently composed this Master thesis and that no other than the indicated aid and sources have been used. This work has not been presented to any other examination board.

04/06/2015

Table of contents

List of acronyms and abbreviations

AICc = corrected Akaike Information Criterion

AFDW = Ash-Free Dry Weight

AODC = Acridine Orange Dapi Count

AWI = Alfred Wegener Institute for Polar and Marine Research

C_{org} = Organic Carbon

CPE = Chloroplastic Pigment Equivalents

d (0.5) = Median grain size

DistLM = Distance-based Linear Model routine

EG = Eastern Greenland sampling station

EGC = Eastern Greenland Current

FDA = Fluorescein Diacetate

J’ = Pielou's evenness index

H’ = Shannon diversity index

HG = HAUSGARTEN sampling station

MIZ = Marginal Ice Zone

MPI = Max Planck Institute for Marine Microbiology

MUC = Multicorer

OM = total Organic Matter

PCA = Principal Component Analysis

RAC = Return Atlantic Current

S = Species richness

SCOC = Sediment Community Oxygen Consumption

TOU = Total Oxygen Uptake

SB = Svalbard islands

TBN = Total Bacterial Number

WSC = Western Spitsbergen Current

YB = Yermak Branch

Executive Summary

The Arctic region is strongly involved in global climate and global cycles of a variety of materials and is therefore important in the present functioning of Earth and its life. It has already been proven that the Arctic pelagic systems are altered by global warming, with a gradual shift towards smaller species in warmer oceans. It is expected that this will propagate through all trophic levels following to the benthic-pelagic coupling. However, what the effects of these pelagic changes will be on the benthic ecosystems remains largely unknown. Furthermore, benthic functioning including organic matter processing, biogeochemistry and the link with environment and bioturbating fauna is still not well understood.

Therefore this study will focus on benthic ecosystem functioning in relation with ice-cover and water depth. Fram Strait is characterised within a small scale by an area with permanent ice-cover in the west and a summer ice-free area in the east. During the sampling campaign "ARK XXVIII-2" on board the RV Polarstern in the period of 6 June to 3 July 2014, information on environmental variables, fauna and biogeochemical fluxes was obtained from both sites along a bathymetric transect. During this study following benthic parameters were determined: concentrations of potential food sources, density and biomass of meio- and macrofauna, total oxygen uptake, bio-irrigation and nutrient fluxes at the sediment-water interface.

A lower food availability was found underneath the multiyear ice and concentrations decreased with increasing water depth. This trend in food concentration was followed by meiofaunal density. Furthermore, macrofauna community composition also differed between the two sites. Both meio- and macrofaunal communities differed at the different water depths. Meiofaunal density was structured by a combination of water depth, chlorophyll and silt percentage. Macrofaunal density was structured by chlorophyll a, while macrofaunal biomass and functional diversity were structured by water depth. Bio-irrigation as well was found to be lower underneath the multiyear ice and was structured by organic matter content. Total oxygen uptake as a part of benthic remineralisation was structured by silt fraction. Nutrient fluxes could not be explained by any of the considered environmental or faunal variables.

Abstract

Although it has been proven that the Arctic is important in the present functioning of Earth and its life and is particularly sensitive to climate change, little is known about benthic ecosystem functioning in the Arctic Oceans. Therefore, to identify the variables structuring benthic functioning, during the summer of 2014 a bathymetric gradient was sampled on both sides of Fram Strait with multiyear ice in the west and a summer ice-free area in the east. The sampled variables included information about the environmental setting, fauna present and biogeochemical fluxes. Ice cover was found to determine the food availability, which in turn affected faunal density, macrofaunal community composition and bio-irrigation rate. In summer ice-free areas underneath the marginal ice zone, food availability was higher and therefore meiofaunal density and bio-irrigation were higher as well. Macrofaunal density was only partly explained by food input and total oxygen uptake as a part of benthic remineralisation was mainly structured by silt fraction in the sediment. Water depth determined faunal community composition, with lower macrofaunal biomass and functional diversity in the deeper areas.

1. Introduction

The Arctic Ocean has been a part of Earth's history over the past 130 My and it contributes significantly to the present functioning of Earth and its life. The Arctic area as a whole (both marine and terrestrial; Fig. 1) forms a heat sink and is important in the formation of both atmospheric and oceanic circulation. Therefore the marine Arctic is strongly involved in global climate and may be important in the global cycles of a variety of materials fundamental to life (Aargaard et al., 1999). However, climate change is nowadays affecting particularly polar systems due to their high sensitivity to increasing seawater temperatures and sea-ice retreat, which together influence food source availability, organismal growth and reproduction, and biogeochemical cycles, but also cause the poleward species migrations (Doney et al., 2012). Therefore it is important to understand the functioning of this specific area in all its aspects.

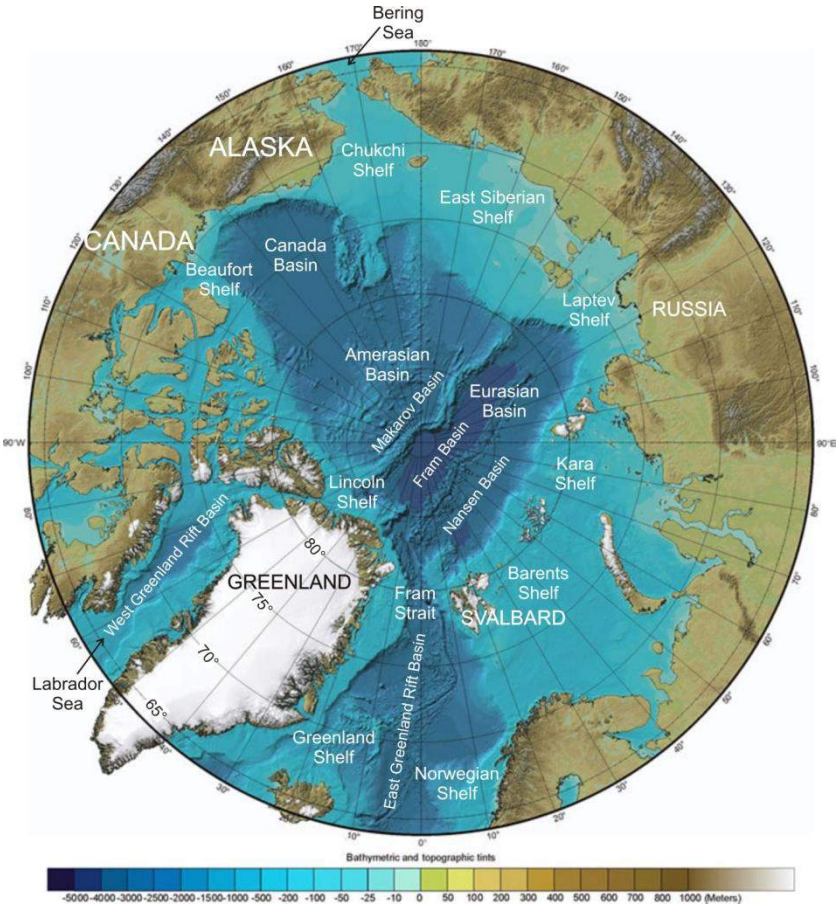

Fig. 1: The Arctic region with indication of both the terrestrial and marine areas. ("Arctic Bathymetric Chart," n.d.)

1.1. Pelagic communities

The marine Arctic is characterised by differences in primary production according to the particular region and its specific setting in terms of hydrography and ice-cover. The ice-covered Central Arctic Ocean (> 80°N; Fig. 1) is characterised by low primary production rates, ranging in the order of 1 to 25 g C m^{-2} yr^{-1} (Arrigo et al., 2008; Boetius et al., 2013; Wassmann et al., 2010). The European sector of the Arctic Ocean, from Fram Strait to the northern Kara Sea (74° - 80°N; Fig. 1), is characterised by ice-covered and ice-free areas and has higher primary production rates of 66 to 89 g C m^{-2} yr^{-1} (Wassmann et al., 2010). Overall, primary production follows the seasonal variation in insolation and nutrient supply (Lalande et al., 2014; Richardson et al., 2005). The annual primary production in the Greenland Sea (Fig. 1) is estimated to be around 70 - 80 g C m^{-2} yr^{-1}; with the onset in March, low production in April (17 mg C m^{-2} d^{-1}), a sharp increase in May and June (800 mg C m^{-2} d^{-1}) and a gradual decrease in July and August (424 mg C m^{-2} d^{-1}) (Richardson et al., 2005). Close to the ice edge, usually higher primary production rates can be found, with an average of ~2000 - 2500 mg C m^{-2} d^{-1} in May and June (Richardson et al., 2005; Smith et al., 1991). The cumulative gross primary production in Fram Strait (Fig. 1) varies from 94 to 123 g C m^{-2} yr^{-1} (Forest et al., 2010), with enhanced primary production (2 - 3 fold of the average) along the marginal ice zone (MIZ). As the MIZ is characterised by a strongly stratified, nutrient-rich euphotic zone, optimal conditions for a bloom are met (Richardson et al., 2005; Sakshaug and Skjoldal, 1989; Schewe and Soltwedel, 2003). Since the Western Spitsbergen Current (WSC) is transporting warm Atlantic Water northward through Fram Strait, ice melting occurs all year round (Spies et al., 1988). Chlorophyll a content in the upper 100 m of the water column was lower in the Eastern Greenland Current in western Fram Strait (EGC; 34 mg/m^2) than in the Western Spitsbergen Current in eastern Fram Strait (WSC; 55 mg/m^2), with different phytoplankton communities in the EGC and the WSC (Nöthig et al., 2014). The onset of the phytoplankton bloom in the WSC occurs in May, while in the EGC the bloom is delayed until July/August (Cherkasheva et al., 2014). Zooplankton communities grazing on this phytoplankton bloom are important in recycling and respiration of the primary production (Møller et al., 2006).

Climate change is expected to increase air temperature in the Arctic region (60° - 90°N) with 2 - 9°C by 2100 (Walsh, 2008). From 2003 to 2006 a warming period was observed, causing increased temperatures of the Atlantic Waters and an enhanced sea ice melting (Bauerfeind et al., 2009; Beszczynska-Möller et al., 2012). As water temperatures rise, fluvial run-off increases and ice cover reduces, ecosystems will change severely, which will propagate through all trophic levels (Hilligsøe et al., 2011; Piepenburg, 2005). Phytoplankton size and community structure are directly

influenced by temperature, next to a nutrient effect, with a gradual shift towards smaller primary producers in warmer oceans (Hilligsøe et al., 2011; Morán et al., 2010). Furthermore, mesozooplankton is related to both temperature and phytoplankton size, with lowest production in warm waters with smallest phytoplankton and shifts itself as well towards smaller species (Hilligsøe et al., 2011; Lalande et al., 2013). It is hypothesised that marine ecosystems will switch in relative importance in the overall carbon and energy flux from 'sea-ice algae – benthos' to 'phytoplankton – zooplankton' dominance, with increased zooplankton grazing responsible for reduced nutrient fluxes to the seafloor and therefore reduced benthic biomass (Piepenburg, 2005).

1.2. Pelagic-benthic coupling

As the patterns and composition of plankton communities change, it can be expected that also the amount, composition and seasonal patterns of sedimenting matter will change (Bauerfeind et al., 2009). In Fram Strait at 300 m water depth, the annual total matter flux varied between 13 and 32 g m^{-2} yr^{-1} (before the warming event of 2005-2006). Minimum fluxes occurred during the winter and maximum fluxes during August/September (Bauerfeind et al., 2009; Lalande et al., 2013). Of this total flux, 4 - 21% could be attributed to refractory particulate organic carbon (POC), 6 - 13% was due to $CaCO_3$ and 3 - 8% to biogenic particulate silicate (bPSi) (Bauerfeind et al., 2009). The sedimenting pattern of the amount of particulate organic matter (POM) remained constant over the years. However, the composition of the flux changed: sedimentation of bPSi decreased as diatoms were partly replaced by coccolithophores; biogenic carbonate (aragonite) concentrations increased as the pteropod community changed to a warm-water species; and fecal pellet carbon (FPC) vertical export reduced as plankton composition decreased in size (Bauerfeind et al., 2009; Busch et al., 2015; Lalande et al., 2013). The seasonal signal of primary and export production from the surface waters is strongly damped at the seafloor (Sauter et al., 2001; Schlüter et al., 2000).

Due to the existence of an efficient retention system and a high degree of recycling within the pelagic food web, less than 10% of the POM produced in the euphotic zone may reach water depths greater than 300 m (Bauerfeind et al., 2009; Forest et al., 2010), while only 2% reaches the seafloor at 1000 m water depth (Schlüter et al., 2000). In the vicinity of the ice-edge though, high concentrations of phytodetritus are present, bPSi and FPC export is always higher and up to 50 - 70% of the pelagic production may reach the bottom. Therefore ice cover is a key factor in determining the frequency and amount of vertical export (Lalande et al., 2013; Sakshaug and Skjoldal, 1989; Schewe and Soltwedel, 2003; Walsh et al., 1985).

1.3. Benthic remineralisation

Due to benthic physical and biological processes, a part of the organic matter (OM) that arrives at the seafloor is recycled and used again for primary production, while another part is buried and lost from the system (Clough et al., 1997). The degradation of OM and coupled oxygen and inorganic nutrient fluxes from the sediments back to the water column, typically in marine soft-bottom environments, is called benthic remineralisation (Jørgensen, 1983; Link et al., 2013a). In polar areas, a tight bentho-pelagic coupling can be found as benthic remineralisation is primarily regulated by the availability of OM and not by temperature (Clough et al., 1997; Morata et al., 2013).

Benthic degradation rate and fluxes in oxygen, carbon and nitrogen decline as water depth increases (Glud et al., 2000). The deep Greenland Sea is characterised by low organic carbon fluxes to the seafloor and is therefore deeply oxygenated (minimal 50 mm deep), with only aerobic mineralisation. A sediment diffusive oxygen flux of 0.2 mmol O_2 m^{-2} d^{-1} was found, which could be related to a seafloor remineralisation of carbon of 0.65 g C m^{-2} yr^{-1} or 1.9 mg C m^{-2} d^{-1} and a degradation rate of 0.004 - 1.1 mg C cm^{-3} yr^{-1} at the sediment surface (Sauter et al., 2001; Schlüter et al., 2000).

1.4. Benthic communities

Benthic communities use OM, arriving at the seafloor, to grow and maintain their population size while respiring the remainder and thereby influence benthic remineralisation (Klages et al., 2004). Benthic communities consist of mega- (> 4 mm), macro- (500 µm - 4 mm), meio- (32 - 500 µm) and microfauna (< 32 µm) (Bodil et al., 2011). In Arctic deep sea sediments, NW of Svalbard, bacteria dominates small sediment-inhabiting organisms (bacteria to meiofauna), with up to 95% and averaged 55% of the total microbial biomass, while meiofauna biomass contributes less than 1% (Soltwedel et al., 2000). In Arctic shelf sediments, at the Barents Sea, oxygen uptake is dominated by microbenthos (57%), followed by macrobenthos (21%), megabenthos (15%) and meiobenthos (7%) (Piepenburg et al., 1995). Also carbon processing in Arctic deep sea sediments, Fram Strait, is dominated by the microbial community with 93%, while meio- (<1%), macro- (1.7%) and megafauna (1.9%) contribute much less (Van Oevelen et al., 2011).

In the shallow Barents Sea, biomass is dominated by megafauna over macro- and meiofauna (Lampitt et al., 1986; Piepenburg et al., 1995). However, all benthic assemblages show a decline in standing stock, both in density and biomass, with increasing water depths, which is even visible within the small scale of Fram Strait. This decline is strongly related to the variations in primary production and

the sedimentation of OM out of the water column, indicating the importance of the bentho-pelagic coupling for the benthos. The quantity and quality of food arriving at the seafloor influences all assemblages, with the microbial production itself furthermore serving as a food source (Bergmann et al., 2011; Górska et al., 2014; Hoste et al., 2007; Meyer et al., 2013; Piepenburg, 2005; Soltwedel and Vopel, 2001; Soltwedel et al., 2009; Wlodarska-Kowalczuk et al., 2004). Due to this depth-related decrease, in body size and biomass, dominance in biomass shifts towards meiofauna and bacteria (Wei et al., 2010) and the relative proportions of bacterial biomass and microbial respiration increase with increasing water depth as well (Soltwedel et al., 2000; Van Oevelen et al., 2011). Furthermore, higher meiofaunal densities are found along the ice edge (Hoste et al., 2007).

1.5. Biological part of benthic remineralisation

Benthic remineralisation is also influenced by the sediment reworking and irrigation activities of macro- and meiofauna (Bonaglia et al., 2014; Braeckman et al., 2010). Therefore, infauna is responsible for transport processes (bioturbation), including both particle reworking and burrow ventilation or solute transfer (bio-irrigation), which makes them also important in oxygen and nutrient cycling (Kristensen et al., 2012). They for example introduce oxygen into the reduced sediments, thereby promoting bacterial oxidation processes, which lead to higher respiration and nutrient release. Therefore this infaunal activity contributes extensively to ecosystem functioning (Bonaglia et al., 2014; Braeckman et al., 2010; Kristensen and Kostka, 2005; Morata et al., 2013).

At the beginning of the winter around 60% of the original OM input is still available, though since this mainly consists of low quality phaeopigments, faunal activities are low (Glud et al., 2000; Morata et al., 2013). It is only after the input of fresh OM, consisting of high quality chlorophyll a, that benthic activities and remineralisation rapidly increase and that benthic fluxes such as oxygen demand and bioturbation become higher (Link et al., 2013b; Morata et al., 2013). Macrobenthic production and carbon demand in the Arctic region therefore reflect the variations in pelagic primary production and thus food availability (Blicher et al., 2009).

1.6. Aims

As outlined above, it is proven that climate change is affecting the Arctic polar region strongly and a basic knowledge of how this is changing the pelagic systems is already obtained. Furthermore it is proven that in the Arctic a very strong pelagic-benthic coupling is existent. However, what the effects of the changing primary production will be on the benthic ecosystems remain largely unknown.

Moreover, as these benthic systems are mainly located in ice-covered deep sea areas, they are hard to study due to practicalities. Therefore they are less understood and basic knowledge on biogeochemistry, organic matter processing and the link with environment and bioturbating fauna is limited. Such investigations have been carried out by Clough et al. (1997) in the central Arctic Ocean and Link et al. (2013b) in the Canadian Arctic, but are lacking for most other areas and were not conclusive. To understand what the effects of climate change on the benthic ecosystems will be and to make predictions, it is necessary to first gain more fundamental knowledge on the present benthic functioning as a whole.

This study will focus on both sides of Fram Strait. In the eastern side of the Strait, the HAUSGARTEN observatory is located in an area with only winter ice. This observatory has been established in 1999 as deep sea, open-ocean, long-term observation station by the German Alfred Wegener Institute for Polar and Marine Research (AWI) in Bremerhaven. The western side on the other hand is still covered by multiyear ice, although this area is reducing in size in response to global warming. Therefore, during this study the impact of ice-cover on benthic communities, benthic remineralisation and benthic ecosystem functioning can be analysed, which has not been done so far. This study will try to relate environmental variables to variations observed in benthic faunal data, but will also try to link this environmental and faunal data to changes in benthic fluxes. This will be done according to different water depths and regions with different ice cover conditions.

The following hypothesis are being tested: (1) meiofaunal and macrofaunal standing stocks decrease with increasing water depth according to decreasing food availability; (2) faunal communities are significantly different at summer ice-free and ice-covered regions according to food availability; and (3) food supply and faunal communities explain the variation in benthic remineralisation functioning.

2. Material and methods

2.1. Study area

Fram Strait, located in the Greenland Sea, forms a large channel (ca. 500 km wide) between northeast Greenland and the Svalbard archipelago (Forest et al., 2010). It is the only deep connection (ca. 2600 m sill depth) between the Arctic and the Atlantic Ocean, with exchange of intermediate and deep waters (Forest et al., 2010; Soltwedel et al., 2005). Two main currents occur in the Strait: the EGC in the west, transporting cold Artic waters (1 °C; <34.4 psu) southward and the WSC in the east, carrying relatively warm and nutrient-rich Atlantic waters (>3 °C; >35 psu) northward (Fig. 2). Between those two along-slope currents, a complex transitional zone is formed, the East Greenland Polar Front (EGPF), with water mixing and recirculation (Forest et al., 2010; Piechura, 2004; Soltwedel et al., 2005). Part of the WSC is recirculated as Return Atlantic Current (RAC; 22%), while the remaining splits up in the Svalbard Branch (SB; 33%) following the Svalbard islands and the Yermak Branch (YB; 45%) flowing along the NW flanks of the Yermak Plateau (Soltwedel et al., 2005). This specific setting results in permanent ice-covered areas in the west, permanent ice-free areas in the southeast, and seasonally varying ice conditions in central and north-eastern parts (Fig. 3) (Soltwedel et al., 2005). The melting of the ice-cover in the central Fram Strait usually begins in June and ice formation expands rapidly in November to reach its maximum in April (Forest et al., 2010; Wlodarska-Kowalczuk et al., 2004).

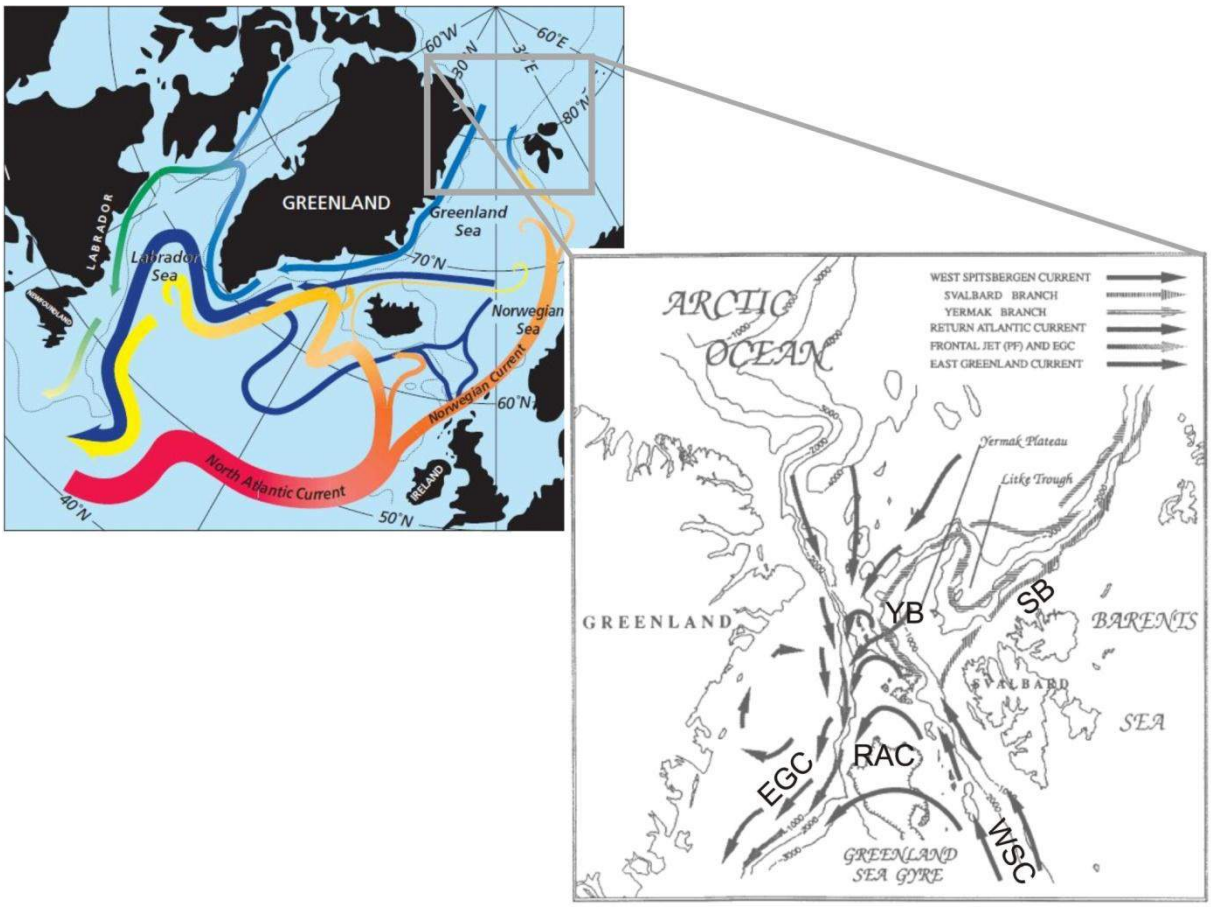

Fig. 2: Oceanographic setting in Fram Strait between Greenland and the Svalbard archipelago. With EGC = East Greenland Current; WSC = West Spitsbergen Current; RAC = Return Atlantic Current; YB = Yermak Branch; SB = Svalbard Branch. (Manley et al., 1992; McCartney et al., 1996)

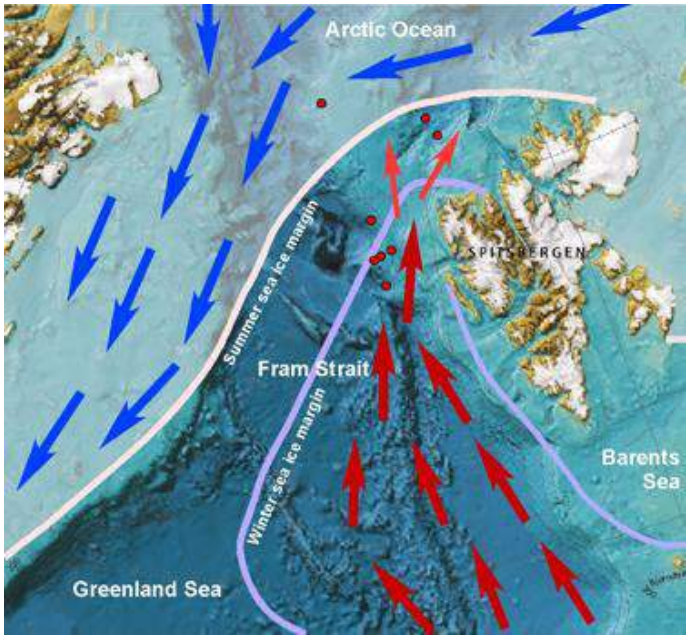

Fig. 3: Extent of summer and winter sea ice in Fram Strait between Greenland and the Svalbard archipelago. (Spielhagen et al., 2015)

2.2. Field Sampling

The sampling campaign on board the RV Polarstern "ARK XXVIII-2" was carried out in the period of 6 June to 3 July 2014. Sampling was done both *ex situ* with a multicorer (MUC) and *in situ* with a Lander equipped with benthic chambers. Eight stations were visited with the MUC and divided in two groups to sample both sides of Fram Strait. Four stations in the EGC (Eastern Greenland sampling stations: EG I to IV) and four stations in the WSC (HAUSGARTEN sampling stations: HG I to IV) (Table 1; Fig. 4). Two of the WSC stations (HG I and IV) were sampled both by the MUC and the Lander. All of the stations were located in a water depth interval between 1000 m and 2500 m. Bottom water temperatures were on average -0.75 °C; bottom water salinity was in all stations 34.9 psu; and bottom water oxygen ranged between 295 µmol/L and 308 µmol/L, which is ~80% saturated. For each station the total benthic exchange of O_2, Br^-, SiO_2, PO_4^{3-}, NH_4^+, NO_3^- and NO_2^- was measured and sediment samples were taken to determine macro- and meiofauna abundances, macrofauna biomass and bacterial abundance. The AWI also took sediment samples from additional MUC cores from the same deployment to analyse for grain size, chlorophyll *a*, phaeopigments, organic carbon, total organic matter and bacterial activity.

Table 1: The eight sampling stations with their geographical position, water depth and bottom oxygen concentration.

Station	Method	Number	Latitude / Longitude	Water Depth	Bottom oxygen concentration (µmol/L)
EG I	MUC	436-1	78° 58. 40'N / 5° 17. 43'W	1059 m	298
EG II	MUC	441-1	78° 56.019'N / 4° 39.020'W	1518 m	300
EG III	MUC	445-1	78° 48.146'N / 3° 52.503'W	1947 m	303
EG IV	MUC	454-3	78°30.350' N / 2°48.995'W	2558 m	302
HG IV	MUC	460-4	79°3.909'N / 4°10.980'E	2418 m	306
HG III	MUC	468-1	79° 6.387'N / 4° 35.087'E	1904 m	308
HG II	MUC	469-2	79° 7.927'N / 4° 54.377'E	1494 m	304
HG I	MUC	470-2	79° 8.011'N / 6° 6.391'E	1245 m	301
HG IV	Lander	457-2	79°3.16'N / 4°8.33'E	2498.6 m	295
HG I	Lander	471-1	79° 8.48'N / 6° 6.99'E	1253 m	302

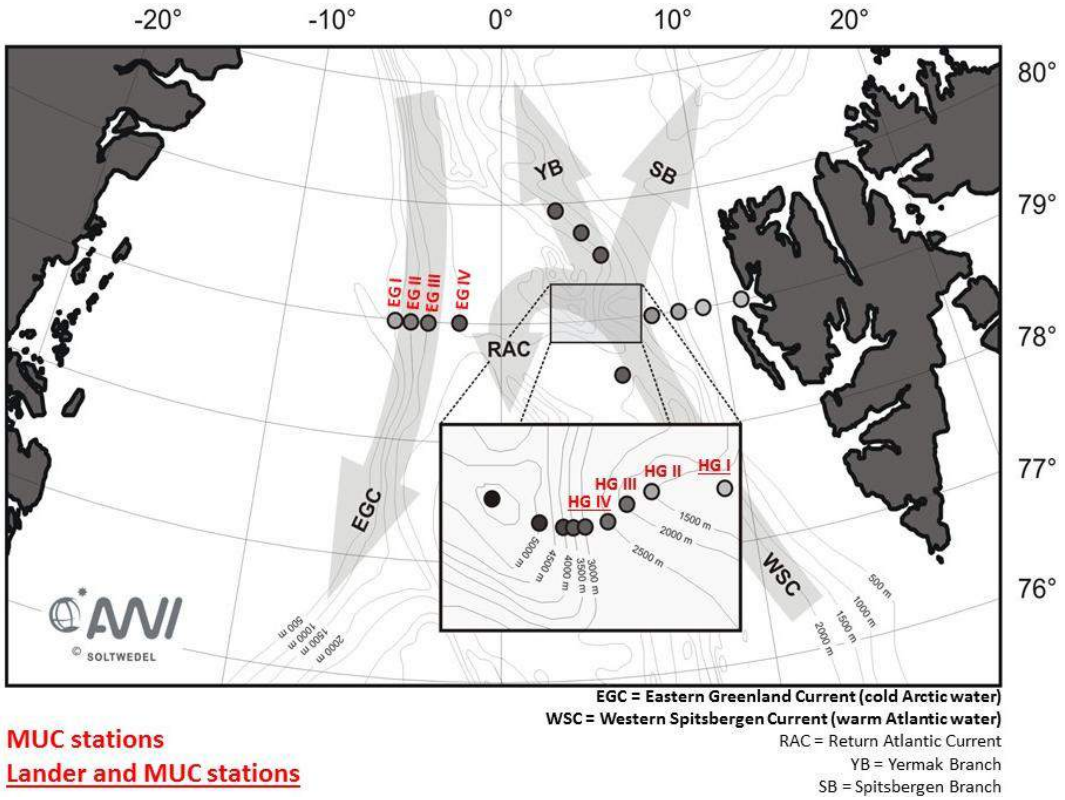

Fig. 4: The eight sampling locations within Fram Strait. Four stations are located in the EGC (EG I to IV) and four in the WSC (HG I to IV). All stations were sampled with the MUC (*ex situ*) and stations HG I and HG IV were additionally sampled with the Lander (*in situ*). All stations were located within a water depth interval from 1000 m (stations I) to 2500 m (stations IV).

Multicorer deployments were used to determine the benthic exchange rates in the laboratory (*ex situ*; Fig. 5a). The MUC retrieved eight sediment cores with overlying water for each sampling station (about 70 cm^2 surface), of which two were available for measuring fluxes at the sediment-water interface. These cores comprised sediment of ~40 cm depth and included therefore the transition between oxic and anoxic strata (1 cm - 5 cm deep at 1000 to 2500 m water depth; Glud, 2008). When incubations were finished, one core was sacrificed for bacterial counts, meiofauna and macrofauna analysis, while the other core was sliced for ^{210}Pb, porosity and density analysis. However, information from the latter core was not yet available for this study.

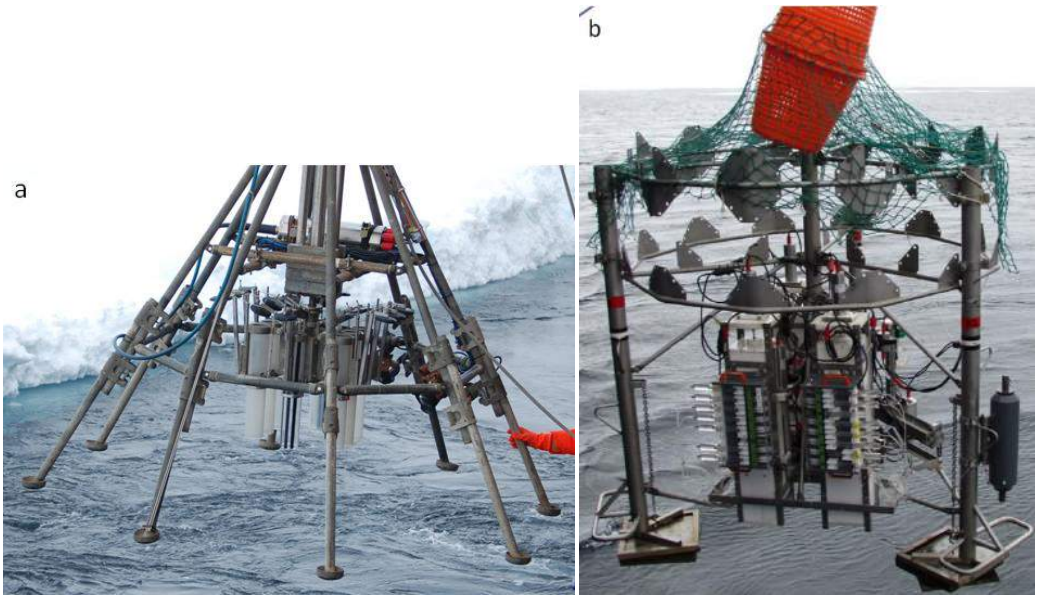

Fig. 5: (a) Multicorer with eight empty sediment cores before deployment. (b) Lander after retrieval, with three full chambers and seven full syringes per chamber.

Lander deployments were used to measure the benthic exchange rates *in situ* (Fig. 5b). The benthic Lander was equipped with three chambers of 20 x 20 cm (400 cm^2 surface), which were pushed into the sea bottom, enclosing a sediment volume of about 8 L (~20 cm sediment depth) and an overlying water volume of about 2-3 L. The incubations ran for 24 hours. An Aanderaa Optode # 4330 from Aanderaa Instruments (Norway) was used to continuously measure the oxygen concentration in the enclosed water. On seven predefined time intervals, syringes were filled with a sample of the overlying water in the chamber. These water samples were used to measure oxygen concentration by Winkler titration as a control measurement for the optode measurements, but also to measure the nutrient concentrations. At the end of the incubation, the chambers were closed from below and the entire chamber incubation (sediment + water) was retrieved from the sea floor. On board, sediment samples were taken to obtain macrofauna and meiofauna samples.

Water measurements from chamber 2 were never usable due to leakage and no oxygen measurements were obtained for chamber 1 at station HG I as the optode was pushed into the sediment. At station HG I, no sediment was retained for chamber 3.

2.3. Sample preparation

After the MUC cores were retrieved on board, they were kept at *in situ* bottom temperature (-0.75 °C). Thirty minutes before the start of the incubation procedure, bromide was added to assess the exchange of solutes across the sediment-water interface. This bromide was added as a NaBr solution of similar density as sea water (1028 g/L). After the bromide addition, the cores were closed

air tight and in each core, the ~10 cm of overlying water was continuously homogenised by a stirring magnet (Fig. 6). Over the total incubation period of ~48 h, oxygen concentration was measured continuously with an Aanderaa Optode # 4330 from Aanderaa Instruments (Norway). At three time intervals (T_0, T_1, T_2), a sample of the water column was taken with a 60 mL syringe. This water volume was replaced by 60 mL of *in situ* bottom water to compensate for the sampled volume in each core. To measure the different concentrations in the water column, the 60 mL sample was subsampled for oxygen, nutrients and bromide (all in triplicates).

After retrieval of the Landers on board, the water samples for the different water column measurements were divided in the same way as for the MUC.

The subsamples for oxygen measurement were stored in a 12 mL Exetainer with glass beads and 120 µL of each Winkler I and II reagent was added. For the nutrient measurements (both MUC and Lander), a subsample was filtered on a GF/F filter and stored in a 10 mL scintillation vial at -20 °C. For the bromide analysis (only MUC), a subsample of 2 mL was kept in an Eppendorf vial and stored at 4 °C. After taking the different water samples, the meiofauna was sampled from the sediment core (both MUC and Lander) with 20 mL syringes until 5 cm sediment depth. These syringes were sliced in one cm resolution and stored in borax buffered formaldehyde solution 4% in Kautex bottles at 4 °C. A subsample was taken for bacterial counts (Acridine Orange Dapi Count; AODC) with a 5 mL syringe, sliced in one cm resolution and stored in a 2% filtered formalin solution at 4 °C. The rest of the core was sieved on a 500 µm mesh to obtain the macrofauna and was stored in borax buffered formaldehyde solution 4%. Data on sediment water content, chlorophyll a, phaeopigments, organic carbon, organic matter and bacterial activity (Fluorescein Diacetate; FDA) were obtained from the Deep Sea Ecology and Technology group at AWI in Bremerhaven.

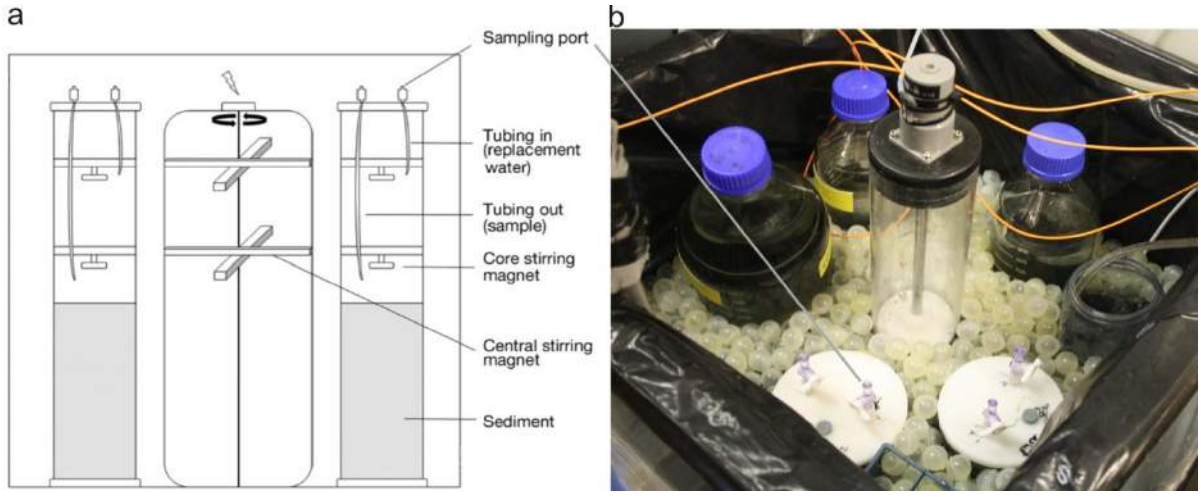

Fig. 6: Set-up for *ex situ* measurements. (a) Schematic overview of a similar set-up from Braeckman et al. (2010) and (b) picture of the incubations on board Polarstern during ARK 28-2.

2.4. Analysis

All oxygen samples were analysed on board within 24h; all nutrient samples and the bromide samples were stored and analysed later at the Max Planck Institute for Marine Microbiology (MPI) in Bremen; the fauna samples were stored and analysed later at Ghent University and MPI. Oxygen was analysed either directly with optodes or with the Winkler method (Parsons et al., 1984) through titration. Nitrate, nitrite, phosphate, ammonium, silicate concentrations were determined using automated colorimetric techniques and bromide concentrations using ion chromatography. All concentrations, except for the optode readings, had to be corrected for the dilution that occurred during the T_1 sampling. Based on the corrected concentration and sampling time, the fluxes could be calculated following: slope of the significant regression of concentration against time * volume of overlying water / sediment surface of the core.

Upon return to the laboratory, the meiofauna samples were sieved on a 500 µm and 32 µm mesh. These two fractions were three times centrifuged in a solution of colloidal silica (Ludox TM-50) with a density of 1.18 g cm^{-3} to extract the fauna from the sediment and were stained with Rose Bengal (Heip et al., 1985). Specimen were counted under a stereomicroscope. Macrofauna samples were immediately stained with Rose Bengal, sieved for a second time on a 500 µm mesh and analysed under a stereomicroscope to pick out, identify and count all specimen.

2.5. Calculations

2.5.1. Environmental variables

All environmental variables, except for Total Bacterial Number (TBN), were given for three replicate cores, from 1 to 5 cm sediment depth in one cm resolution. Median grain size (d (0.5); µm), silt fraction (%), water content (%), total organic matter (OM; %), organic carbon (C_{org}; %) and Fluorescein Diacetate (FDA – bacteria enzymatic activity; nmol/mL/h) are calculated as averages over the sediment depth. Chlorophyll a (µg/L), phaeopigments (µg/L), Chloroplastic Pigment Equivalents (CPE; µg/L) and Ash-Free Dry Weight (AFDW; µg) are calculated as the sum over the sediment depth. Data on the TBN (cell number/mL sediment) is given as 60 replicate AODC counts (Acridine Orange Dapi Count) from 0-1 cm sediment depth. Therefore TBN is calculated as the average of these 60 replicate counts. These above mentioned environmental variables were only measured for the MUC stations and therefore representation only includes these stations. All results were represented along the bathymetric gradient as sum or average over the sediment depth and average over the replicates ± the standard error.

2.5.2. Biogeochemical variables

Oxygen flux was calculated based on the optode data, however when not available, the flux was calculated from the Winkler data. A dilution correction is necessary for the calculation of the fluxes of oxygen (from Winkler titration), nitrate, nitrite, phosphate, ammonium, silicate and bromide; since replacement water with the same concentrations as at T_0 is used to replace the sampled volume. Therefore the concentration from T_1 onwards gets diluted with 10% of the volume and from T_2 onwards, the following correction has to be applied: the corrected concentration is calculated from the concentration of the replacement water, the concentration before correction, the volume of replacement water and the total water volume:

Station	Time	Replicate	Sampling time (d)	Water volume (L)	Surface (m^2)	Measured [Br] (mmol/l)	Dilution	Corrected [Br] (mmol/l)
PS85/445-1	0	A	0.3000	0.6819	0.0071	5.5009		5.5009
PS85/445-1	0	B	0.3000			5.4555		5.4555
PS85/445-1	0	C	0.3000			5.5560		5.5560
PS85/445-1	1	A	1.5535			4.6980		4.6980
PS85/445-1	1	B	1.5535			4.6929		4.6929
PS85/445-1	1	C	1.5535			4.7772		4.7772
PS85/445-1	2	A	2.5278			4.5207	-0.3636	4.1571
PS85/445-1	2	B	2.5278			4.5171	-0.3633	4.1538
PS85/445-1	2	C	2.5278			4.5721	-0.3682	4.2040

REPLACEMENT WATER

Station	Time	Replicate	Sampling time (d)	Measured [Br] (mmol/l)	Average [Br] (mmol/l)
PS85/445-1	1	A	1.5451	0.4059	**0.3880**
PS85/445-1	1	B	1.5451	0.3993	
PS85/445-1	1	C	1.5451	0.3589	

② =[average Br (0.3880) - Br (4.5721)] * volume replaced (0.06) / water volume (0.6819)

③ =Br (4.5721) + dilution (-0.3682)

① = average of Br (0.4059+0.3993+0.3589)/3

Based on these corrected concentrations, the fluxes can be calculated. Therefore first the slope of the concentration over time needs to be calculated:

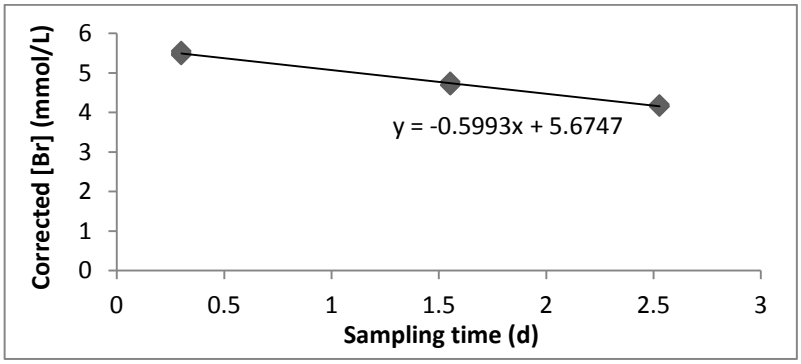

From this slope, the water volume and the sediment surface, the final flux can be determined:

slope (mM/d) -0.5993 ← from graph (corrected Br versus sampling time)

flux (mmol/m²/d) -57.6527 ← = slope (-0.5993 mmol/L/d) * water volume (0.6819 L) / surface (0.0071 m^2)

Finally, the significance of the regression of these fluxes has to be checked, which was done in R v3.2.0. (R Core Team, 2015). First of all, the residuals should be smaller than three times the standard deviation to make sure no outliers are present in the data. Next, a permutation test (999 permutations) was executed to check the significance of the regression. When the regression was significant ($p < 0.05$), a linear model was fitted to the samples. Otherwise the flux became zero as there was no significant change over time. In case there was an indication of a sampling or analysis error, these fluxes were not withheld. Bromide fluxes were only measured for the MUC stations. All fluxes were represented along the bathymetric gradient.

2.5.3. Faunal variables

After meiofauna and macrofauna specimen were counted and macrofauna was weighted, numbers had to be recalculated to standard surface. Meiofauna was sampled with a syringe of 20 mm diameter and was therefore counted as number of individuals/3.1415 cm^2. Meiofauna density had to be represented as ind./10 cm^2. Macrofauna was sampled with a 95 mm MUC core and a 20 cm x 20 cm Lander chamber. Therefore MUC samples were counted as number of ind./0.007088 m^2 and weighted as mg/0.007088 m^2, and Lander samples as ind./0.04 m^2 and mg/0.04 m^2. Macrofauna density had to be represented as ind./m^2 and biomass as mg/m^2.

Meiofauna counts were done for each station over a 5 cm sediment depth interval, with a one cm resolution. No counts could be obtained for slice 1-2 cm sediment depth at 1253 m water depth for Lander_HG1_K1. The sum over the sediment depth was represented along the bathymetric gradient, with average over the replicates ± the standard error for the Lander stations.

Macrofauna counting and weighting were done over the whole core. Representation was again done along the bathymetric gradient, with average over the replicates ± the standard error for the two Lander stations. For further analysis, all cores at the Lander stations were withheld separately.

From the macrofauna density (A_i) and biomass (B_i), together with a mobility (M_i) and sediment reworking (R_i) score of each species, the community bioturbation potential (BPc) can be calculated (Queirós et al., 2013). Calculation is done according to following formula:

$$\mathrm{BP_c} = \sum_{i=1}^{n} \sqrt{\mathrm{B}i/\mathrm{A}i} \times \mathrm{A}i \times \mathrm{M}i \times \mathrm{R}i$$

With i = specific species/taxon in the sample.

This index is calculated for all MUC stations and all Lander cores. The results were again represented against the bathymetric gradient, with indication of the standard error for the Lander stations.

2.6. Data analysis

Since environmental variables (grain size, chlorophyll *a*, phaeopigments, CPE, C_{org}, water content, AFDW, OM, TBN and FDA) were only available for the MUC stations, Lander stations were excluded from all analyses including this environmental data. Otherwise, when using faunal and/or biogeochemical data without environmental data, both MUC and Lander stations were included. Before using any explanatory variables in any analysis, these variables were first normalised within PRIMER v6. A Principal Component Analysis (PCA) and Draftsman correlation matrices were performed in PRIMER v6 to visualise any patterns in the environmental, biogeochemical and faunal data.

Species richness (S), Pielou's evenness index (J') and Shannon diversity index (H') were calculated for the meio- and macrofauna data and represented along the bathymetric gradient. Since meiofauna data was dominated by nematodes, an overall square root transformation was performed. As no single dominant species could be detected in the macrofauna community, there was no need to transform the data. Analysis of meiofauna densities was both done on the original and the transformed data. One-way ANOSIM tests performed on the Bray-Curtis similarity matrix were used to test for significant differences in community structure between the water depth classes and sampling sites (EG versus HG). Next, a one-way SIMPER analysis was performed to assess the dissimilarity between the different water depth classes and sites. The relation between the normalized Euclidian distance similarity matrix of the environmental variables and Bray-Curtis similarity matrix of the faunal data was analysed using the RELATE procedure with spearman correlation. To define the environmental variables best explaining faunal structure, the BIO_ENV procedure with Spearman correlation was used with the normalized environmental data and the Bray-Curtis similarity matrix of the faunal data.

The relationship between the faunal composition and the explanatory variables (environmental data) was investigated using the Distance-based Linear Model routine (DistLM) in PERMANOVA+. Prior to this analysis, the following non-normally distributed variables were log transformed: d (0.5), silt percentage, chlorophyll a, phaeopigments, CPE, AFDW, water content, OM, FDA and TBN. After transformation, correlation had to be checked, as all correlated variables had to be excluded from the analysis. This was assessed using the Draftsman correlation matrix with a threshold of correlation $r > 0.8$. The analysis was performed with the BEST selection procedure and the AICc selection criterion (corrected Akaike Information Criterion) on different sets of non-correlated predictors. First, each predictor was analysed separately with the marginal test. Next, the BEST procedure also gave

an indication of the overall best model and finally a sequential test was used as well. All analysis on fauna was performed within PRIMER v6 with the PERMANOVA+ add-on (Anderson et al., 2008; Clarke and Gorley, 2006), with significance level of $p<0.05$ based on 999 permutations (where possible). The relationship between BPc and site (EG versus HG) was analysed with the parametric t-test in R v3.2.0.

The relation between the biogeochemical fluxes and site (EG versus HG) was analysed. For oxygen data, the parametric t-test in R v3.2.0 was used. For the other fluxes (bromide, silicate, phosphate, ammonium, nitrite + nitrate and nitrite), the non-parametric Kruskal-Wallis test in R v3.2.0 was used, since assumptions for parametric tests (normality and homogeneity) were not met for these variables. The relationship between the biogeochemical fluxes and the explanatory variables (faunal composition and environmental data) was investigated using the DistLM routine in PERMANOVA+. For details see above. However, no sequential test was used during this analysis. The following variables were log transformed: d (0.5), silt percentage, chlorophyll a, phaeopigments, CPE, AFDW, water content, OM, FDA, TBN, meiofaunal density, nematode density, macrofaunal density, crustacean density, mollusc density, macrofaunal biomass, polychaete biomass, crustacean biomass, mollusc biomass and BPc. This analysis was performed within PRIMER v6 with the PERMANOVA+ add-on (Anderson et al., 2008; Clarke and Gorley, 2006).

The chosen best model, was the model with the highest explanatory strength within a 2 units range of the smallest AICc. Since the AICc indicates the amount of information lost, the model with the smallest AICc value is preferred. Furthermore, models deviating within a 2 units range from the smallest AICc value receive substantial support, everything outside this 2 units range is considered to have considerably less support (Burnham and Anderson, 2003; Posada and Buckley, 2004).

3. Results

3.1. Environmental variables

Over the bathymetric gradient, the median grain size (0-5 cm averaged) ranges between 13 µm and 23 µm, with the exception of the deepest station (EG IV: 88 µm). This is well within the boundaries of the silt fraction of 4 - 63 µm (Table 2; Fig. 7a). Silt forms the dominant grain size, ranging from 48% at the deepest EG station to 97% at the shallowest EG station (Table 2; Fig. 7b). Overall, the shallowest stations (1000 m water depth class) have the finest sediments and the deepest (2500 m water depth class) have the coarsest sediments (Fig. 7).

The water content (0-5 cm averaged) of the sediments decreases with water depth and is highest at the eastern side of the strait (Table 2; Fig. 8).

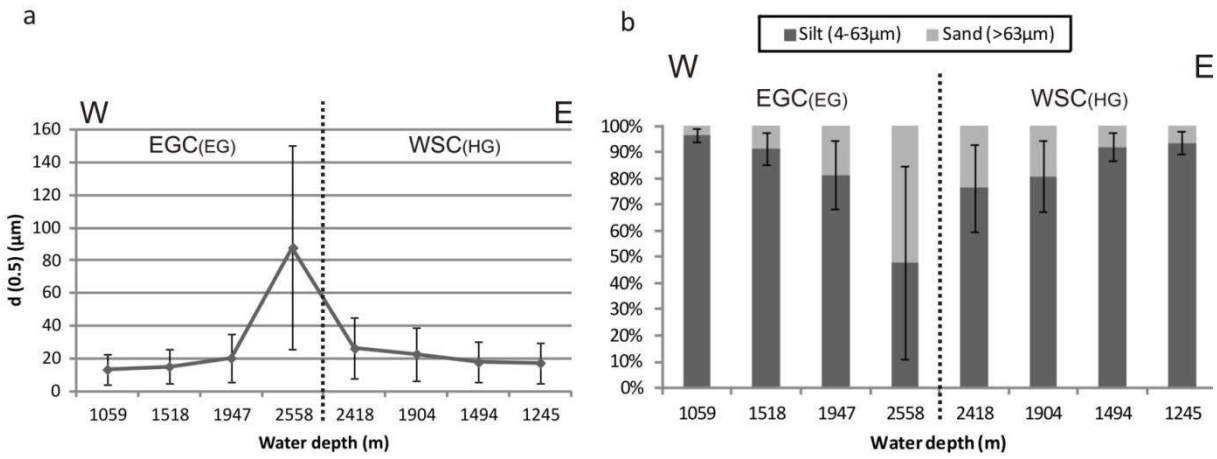

Fig. 7: (a) Average median grain size of the sediment (0-5 cm) over the bathymetric gradient in Fram strait. (b) Average sediment grain size fractions of silt and sand (0-5 cm) over the bathymetric transect. Standard error is based on the three replicate cores.

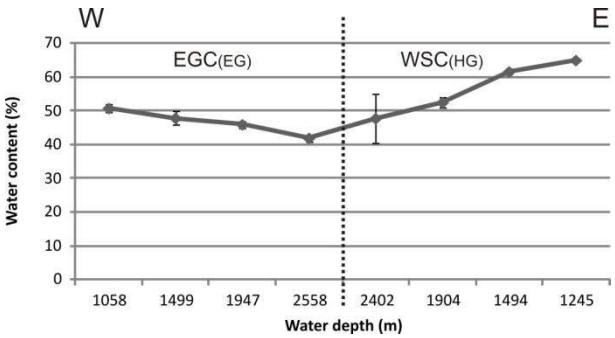

Fig. 8: Averaged water content of the sediment (0-5 cm), with standard error based on the three replicate cores.

Overall, the sediment-bound chloroplastic pigment concentrations (Chlorophyll a and Phaeopigment a; 0-5 cm summed) were low in the western side of the strait (Table 2; Fig. 9a). These

pigment concentrations gradually increased towards the east and shallower water depths. Over the whole transect, the degraded phaeopigment was dominant over the fresh chlorophyll.

The organic carbon concentrations (0-5 cm averaged) show the same trend, with low concentrations in the western part of the strait and an increase towards the east and shallower water depths (Table 2; Fig. 9b).

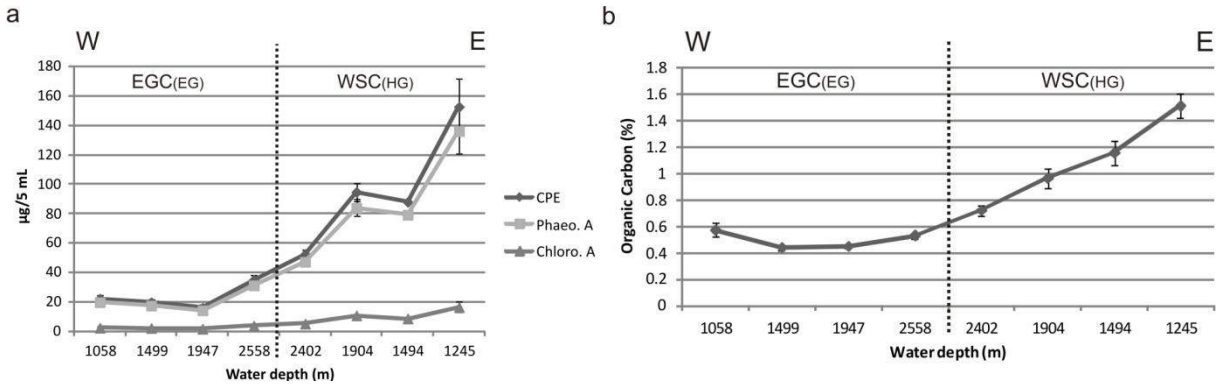

Fig. 9: (a) Summed chloroplastic pigment concentrations (0-5 cm) along the bathymetric transect; with CPE = Chloroplastic pigments equivalent, Phaeo. A = Phaeopigment a and Chloro. A = Chlorophyll a. (b) Average percentage of organic carbon (0-5 cm) along the transect. Standard error is based on the three replicate cores.

AFDW (0-5 cm summed), an estimation of total organic content, shows no trend with water depth, but displays the highest concentration at station HG III at 1904 m water depth (Table 2; Fig. 10a).

The organic matter concentrations (0-5 cm averaged) show the same course as AFDW (Table 2; Fig. 10b).

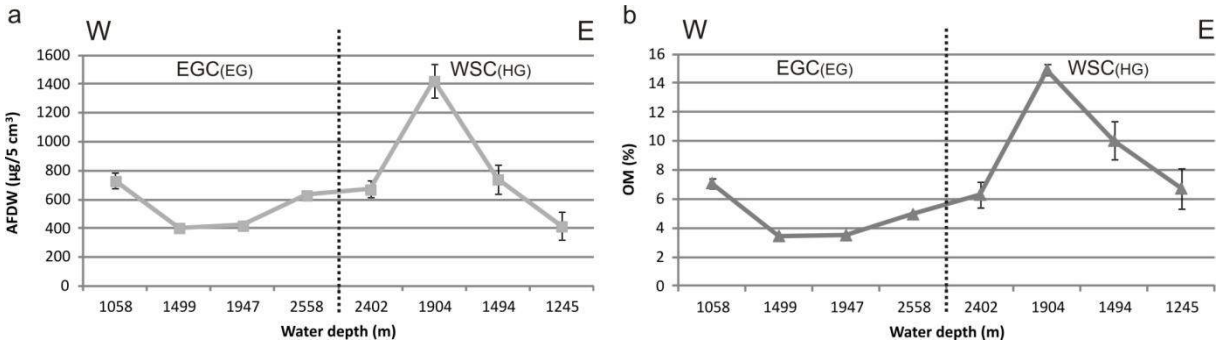

Fig. 10: (a) Summed Ash-free Dry Weight = AFDW and (b) averaged percentage of total organic matter = OM in the sediment (0-5 cm) over the transect. Standard error is based on the three replicate cores.

Bacterial enzyme activity (FDA; 0-5 cm averaged), an estimate for bacterial turnover, shows the same trend as the chloroplastic pigment concentrations and C_{org}: low enzyme activity in the west and increasing activity towards the east and shallower stations (Table 2; Fig. 11a).

Total bacterial number (0-1 cm) on the other hand shows a decrease towards the deeper stations, with a single peak at station EG IV at 2558 m water depth and overall highest abundance at the two shallowest HG stations (Table 2; Fig. 11b).

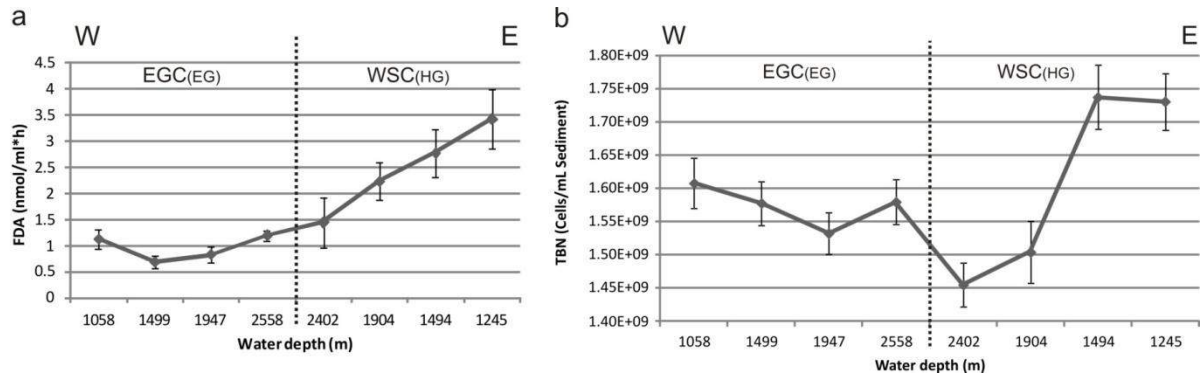

Fig. 11: (a) Averaged Fluorescein Diacetate = FDA (= bacterial enzyme activity) (0-5 cm), with standard error based on the three replicate cores and (b) Total Bacterial Number = TBN at the 0-1 cm sediment depth along the transect.

Though some environmental factors showed some trend with water depth, only silt is correlated with water depth class (r = -0.83) (Appendix Table 1). FDA is correlated with all three pigment concentrations (r of the three concentrations ≈ 0.97), C_{org} content (r = 0.99) and water content (r = 0.90). The ANOSIM results showed that the environmental variables are significantly different between the two sites (R = 0.581 and p = 0.001), but not at the different water depth classes (R = 0.104 and p = 0.08).

Table 2: Environmental data (0-5 cm averaged or summed and 0-1 cm for TBN) from sampling sites along the bathymetric gradient. With d (0.5) = median grain size; Chl a = chlorophyll a; Phaeo = phaeopigment a; CPE = chloroplastic pigments equivalent; C-org = organic carbon; AFDW = ash-free dry weight; WC = water content; OM = total organic matter; FDA = fluorescein diacetate; TBN = Total Bacterial Number. For each of the variables the standard error (SE), based on the average of the three replicate cores, is indicated in grey.

Station	Depth (m)	d (0.5) (µm)	SE	Silt (%)	SE	Chl a (µg/ 5 mL)	SE	Phaeo (µg/ 5 mL)	SE	CPE (µg/ 5 mL)	SE	C-org (%)	SE	AFDW (µg/ 5 cm^3)	SE	WC (%)	SE	OM (%)	SE	FDA (nmol/ mL*h)	SE	TBN (Cells/mL Sediment)	SE
MUC_EG I	1059	13.38	9.46	96.51	2.47	2.25	0.42	18.36	2.16	20.60	2.45	0.57	0.05	731.13	52.97	50.76	1.16	7.10	0.36	1.13	0.19	1.61E+09	3.73E+07
MUC_EG II	1518	15.11	10.68	91.42	6.07	2.10	0.26	16.26	1.58	18.36	1.80	0.44	0.02	405.66	16.87	47.87	2.03	3.45	0.05	0.69	0.11	1.58E+09	3.33E+07
MUC_EG III	1947	20.33	14.37	81.43	13.13	1.59	0.36	13.24	1.78	14.83	2.14	0.45	0.01	421.69	15.85	45.95	0.91	3.51	0.03	0.83	0.15	1.53E+09	3.20E+07
MUC_EG IV	2558	87.98	62.21	47.76	36.94	3.62	0.84	29.36	2.51	32.98	2.85	0.53	0.02	632.12	15.02	41.93	1.00	4.96	0.14	1.20	0.10	1.58E+09	3.31E+07
MUC_HG IV	2418	26.29	18.59	76.54	16.59	4.86	0.60	44.05	2.27	48.91	2.81	0.72	0.04	672.17	57.74	47.76	7.22	6.31	0.89	1.45	0.47	1.46E+09	3.34E+07
MUC_HG III	1904	22.85	16.16	80.85	13.54	10.01	0.42	77.89	5.29	87.91	5.67	0.97	0.07	1425.14	117.92	52.49	1.54	14.92	0.40	2.23	0.36	1.50E+09	4.66E+07
MUC_HG II	1494	17.79	12.58	92.15	5.55	7.99	0.27	72.64	0.80	80.63	0.92	1.16	0.09	743.23	101.37	61.61	0.74	10.03	1.32	2.77	0.46	1.74E+09	4.84E+07
MUC_HG I	1245	17.35	12.27	93.66	4.48	15.04	3.33	124.37	14.31	139.41	17.50	1.51	0.09	416.81	96.28	64.99	0.66	6.74	1.39	3.42	0.56	1.73E+09	4.30E+07

Three main groups can be distinguished from the PCA plot (Fig. 12): (1) EG from 1000 m to 2000 m water depth on the right side of the plot, (2) HG from 1000 m to 2000 m water depth on the left side, and (3) the deep station at 2500 m water depth from both EG and HG sites right below. Principle component 1 is correlated with organic carbon concentration (r = -0.376), the pigment concentrations (r of the three concentrations ≈ -0.38) and FDA (r = -0.366), and explains 50.0% of the variation. The second component is correlated with the water depth class (r = -0.470) and grain size (median and silt, r ≈ 0.49), and only explains 19.4%. EG 1000 m to 2000 m water depth can be separated from HG 1000 m to 2000 m water depth by PC1. Shallow water depths of 1000 m and 1500 m can be distinguished from deep water depths of 2000 m and 2500 m by PC2. The deepest stations from both EG and HG can be separated from the other stations by a combination of PC1 and PC2. Therefore, organic carbon, pigments and FDA explain almost 50% of the variation between the 2 sites (EG or HG), while water depth and grain size explain almost 20%.

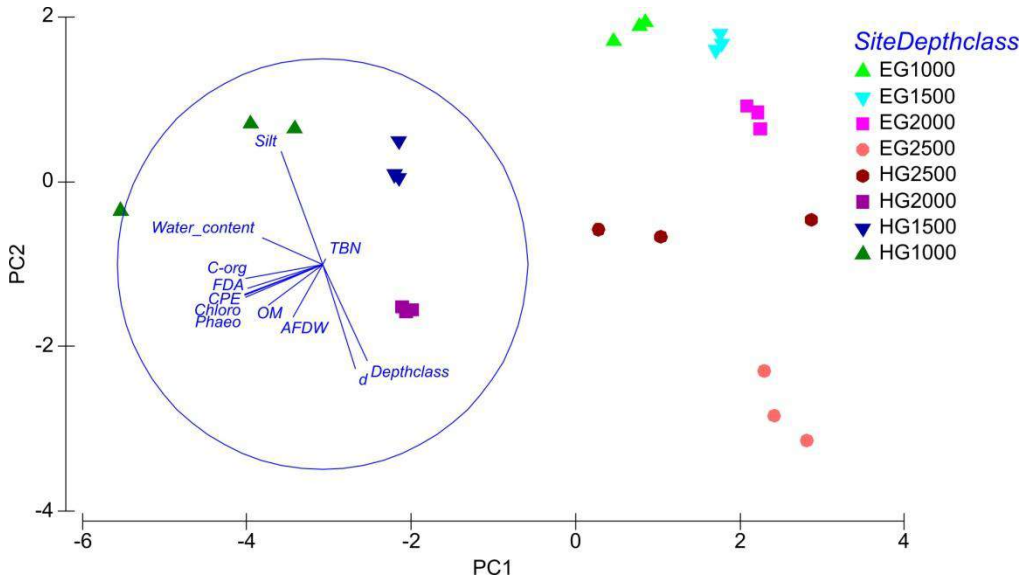

Fig. 12: PCA plot including all environmental variables (Depthclass = water depth class; d = median grain size; Chloro = chlorophyll a; Phaeo = phaeopigment a; CPE = chloroplastic pigments equivalent; C-org = organic carbon; AFDW = ash-free dry weight; WC = water content; OM = total organic matter; FDA = fluorescein diacetate; TBN = total bacterial number). Samples are plotted according to their position in Fram strait (EG-HG) and their water depth (1000 m to 2500 m). PC1 explains 50.0% of the variation and PC2 19.4%.

3.2. Faunal communities

3.2.1. Meiofauna

A total of 2196 metazoan meiobenthos organisms were counted, belonging to 12 major taxa. Mean meiobenthos densities for each station are given in Table 3 and Fig. 13. Species richness per sample area ranged between 2 (EG III at 1947 m water depth) and 8 taxa (HG I at 1245 m water depth) per station (Table 3). Nematodes were in all stations the most abundant taxon (88 - 98%). Copepods were the second most abundant group (1 - 8%) and nauplii the third group (0 - 5%). The other taxa consisting of polychaetes, kinorhynchs, ostracods, oligochaetes, priapulid worms, tanaidaceans, nemerteans, sipunculids and poriferans were found in much lower abundances. Mean meiobenthos and nematode densities along the bathymetric transect are shown in Fig. 13. Mean meiofaunal densities ranged between 137 ind. 10 cm^{-2} (EG III: 1947 m) to 1611 ind. 10 cm^{-2} (HG I: 1245 m) (Table 3) and nematode density ranged from 134 nematodes 10 cm^{-2} (EG III: 1947 m) to 1410 nematodes 10 cm^{-2} (HG I: 1245 m) (Table 4). Pielou's evenness index (J') shows that meiofauna within stations is never even (J' < 0.5), but that EG stations are generally less uneven than HG stations (Fig. 14). The Shannon diversity index (H') shows that meiofauna diversity is low overall, but EG stations and the shallowest HG station have a higher diversity than the others. Furthermore, both indices indicate that station EG III at 1947 m water depth has a lower evenness and diversity than the other EG stations and is comparable to the deeper HG stations (Fig. 14).

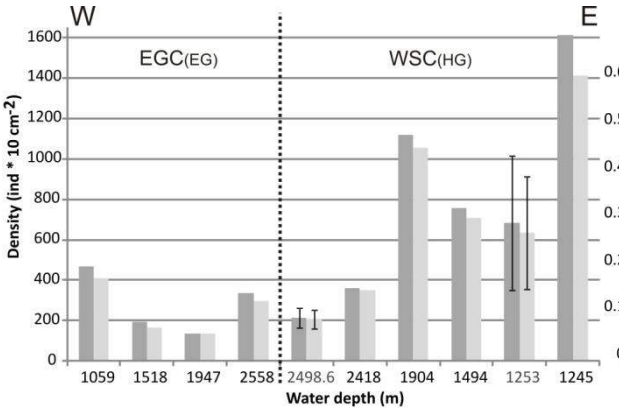

Fig. 13: Average meiofauna density (dark grey) and nematode density (light grey) in the upper 5 cm of the sediment, over the bathymetric gradient. The Lander stations are indicated by the error bars and grey water depth labels.

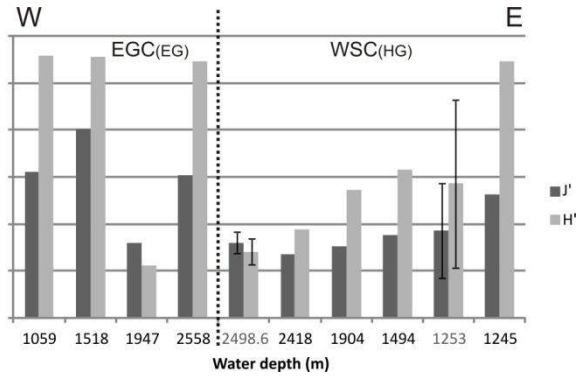

Fig. 14: Pielou's evenness index (J') and Shannon diversity index (H') (0-5 cm) over the transect. The Lander stations are indicated by the error bars and grey water depth labels.

No correlation exists between meiobenthos nor nematode density and water depth (Appendix Table 2). However, meiobenthos and nematode density are correlated with each other (r = 1) and with the environmental variables pigment concentrations (r of the three concentrations ≈ 0.96), organic carbon content (r = 0.93), water content (r = 0.82) and FDA (r = 0.92)(Appendix Table 3).

Meiobenthos communities were only significantly different between the four water depth classes (1000 m, 1500 m, 2000 m and 2500 m water depth) (ANOSIM R = 0.322 and p = 0.045). No significant differences could be found among sites (EG-HG). The pairwise test pointed out that the difference occurs between 1000 m and 2500 m water depth. SIMPER analysis resulted in highest dissimilarity of 48.30% between 1000 m and 2000 m water depth. 1000 m and 2500 m water depth displayed a lower dissimilarity of 46.43%, similar to the dissimilarity of 46.07% between 2000 m and 2500 m water depth. The Bray-Curtis similarity matrix of the meiofaunal densities could significantly be related through Spearman correlation to the normalized Euclidian distance similarity matrix of the environmental data (R = 0.591 and p = 0.004). Using the BIO_ENV procedure with the Spearman correlation, chlorophyll a + OM + FDA could explain the variation in the meiobenthos community composition data best (R = 0.83 and p = 0.006).
However, when square root overall transformation was used on the meiofaunal community data to correct for the nematode dominance, results became different. ANOSIM results indicated significant difference between the water depth classes (R = 0.37 and p = 0.02). The pairwise test pointed out that the difference occurs between 1000 m and 2500 m, and 1500 m and 2500 m water depth. SIMPER analysis indicated greatest dissimilarities between 1000 m and 2000 m water depth (37.64%) and between 1000 m and 2500 m water depth (37.28%). Relating the meiofaunal and environmental similarity matrices became non-significant (R = 0.354 and p = 0.058), as did the BIO_ENV procedure (R = 0.578 and p = 0.108).

The draftsman correlation plot with log transformed variables, on which the exclusion of correlated variables for the DistLM analysis was based, is shown in Table 8.
The DistLM analysis showed that meiofaunal density is best explained by 85% by a combination of chlorophyll (p = 0.014) with depth class (p = 0.043) and silt (p = 0.414) (AICc = 18.174). However, all three variables were found to be significant using the sequential test (chlorophyll: p = 0.018; depth class: p = 0.046; silt: p = 0.009). The exact same result could be found when only nematode density was considered. The overall best model (AICc = 36.239) explaining 84% of the variability was again indicated to be a combination of chlorophyll (p = 0.021) + depth class (p = 0.057) + silt (p = 0.479). However, all three variables were found to be significant using the sequential test (chlorophyll: p = 0.025; silt: p = 0.033; depth class: p = 0.004).

Table 3: Faunal data (0-5 cm) from sampling sites along the bathymetric gradient. Meiofauna density, macrofauna density, macrofauna biomass and community bioturbation potential (BPc), as well as meiofaunal and macrofaunal species richness per sample area (S). Sample area for meiofauna = 0.00031415 m^2 and 0.007088 m^2 for MUC macrofauna and 0.04 m^2 for Lander macrofauna. The Lander stations are denoted with their standard error (SE).

Station	Depth	Meiofauna				Macrofauna				Macrofauna		BPc	SE
	(m)	Density (ind*10 cm^{-2})	SE	S	SE	Density (ind*m^{-2})	SE	S	SE	Biomass (mg*m^{-2})	SE		
MUC_EG I	1059	468		6		1411		6		3524.16		634	
MUC_EG II	1518	194		4		988		7		1970.88		291	
MUC_EG III	1947	137		2		282		2		1300.75		86	
MUC_EG IV	2558	337		6		1693		8		450.04		109	
MUC_HG IV	2418	363		4		564		4		100.17		18	
MUC_HG III	1904	1117		6		1552		11		1247.14		215	
MUC_HG II	1494	754		6		1552		7		1149.8		152	
MUC_HG I	1245	1611		8		1552		11		3820.42		239	
LANDER_HG IV	2498.6	214	50	3	0.82	417	101	9	1.22	836.17	436.23	60	23
LANDER_HG I	1253	683	331	5	0.71	988	442	15	7.78	6929	1365.78	337	61

Table 4: Meiofaunal densities (individuals/10 cm^2) per taxa for each station. With standard error for the Lander stations.

Station	Depth	Nematode	Copepode	Nauplii	Polychaete	Kinorhyncha	Ostracode	Oligochaeta	Priapulida	Tanaidacea	Nemertea	Sipunculida	Porifera
MUC_EG I	1059 m	411	13	16	13	13	3	0	0	0	0	0	0
MUC_EG II	1518 m	166	16	3	0	0	10	0	0	0	0	0	0
MUC_EG III	1947 m	134	3	0	0	0	0	0	0	0	0	0	0
MUC_EG IV	2558 m	296	13	16	6	0	3	0	0	0	0	0	3
MUC_HG IV	2418 m	350	3	0	6	0	0	3	0	0	0	0	0
MUC_HG III	1904 m	1057	10	38	3	3	6	0	0	0	0	0	0
MUC_HG II	1494 m	707	19	19	0	0	3	0	3	0	3	0	0
MUC_HG I	1245 m	1410	92	64	16	16	6	0	0	3	0	3	0
LANDER_HG IV	2498.6 m	208±47	3±2	0±0	2±1	0±0	1±1	0±0	0±0	0±0	0±0	0±0	0±0
LANDER_HG I	1253 m	633±279	21±29	18±20	8±2	0±0	2±2	2±2	0±0	0±0	0±0	0±0	0±0

3.2.2. Macrofauna

In total, 197 macrobenthos organisms from 7 major taxonomic groups were counted, with a total biomass of 29929.85 mg. Mean macrobenthos densities and biomass for each station are given in Table 3 and Fig. 16 & 17. Table 3 also displays the species richness per sample area per station, ranging between 2 (EG III at 1947 m water depth) and 15 (HG I at 1253 m water depth). Polychaetes formed the most important taxon (10 - 55%), but they were absent at station EG II at 1518 m water depth. The second most important taxon was formed by the molluscs (9 - 51%), which were absent in stations EG III at 1947 m and HG II at 1494 m water depth. The third taxon, crustaceans (8 - 50%) were absent from station HG IV at 2418 m water depth. According to biomass, molluscs formed the most important taxon (1 - 60%), second most important were the crustaceans (1 - 93%) and third became the polychaetes (5 - 94%). The other taxa (anthozoans, nematodes, nermerteans and sipunculids) appeared in much lower densities and biomass. Mean macrobenthos density and the cumulated densities of the three most important groups (polychaeta, crustacea and molluscs) are shown in Fig. 16. The mean macrobenthos biomass and the cumulated biomass of the three major taxa are displayed in Fig. 17. Mean macrobenthos densities ranged from 282 ind. m^{-2} (EG III: 1947 m) to 1693 ind. m^{-2} (EG IV: 2558 m) and biomass ranged between 100 mg m^{-2} (HG IV: 2418 m) to 6929 mg m^{-2} (HG I: 1253 m) (Table 3). The densities and biomasses for the major groups per station are shown in Table 5 & 6. Pielou's evenness index (J') is always close to 1 and indicates therefore a high evenness in all stations (Fig. 18). The Shannon diversity index (H') shows an overall higher diversity than for meiofauna, with the highest diversities at HG III (1904 m) and HG I (1245 m) and the lowest diversity at EG III (1947 m)(Fig. 18).

Macrobenthos density has no correlation with any environmental variable, while macrobenthos biomass is correlated with water depth class ($r = 0.82$) and mollusc biomass ($r = 0.91$) (Appendix Table 2 & 3). Mollusc biomass is correlated with both median grain size and silt percentage ($r = 0.91$ and $r = -0.83$).

BPc is highest at station EG I at 1059 m water depth with a value of 634 and lowest at station HG IV at 2418 m with a value of 18 (Table 3; Fig. 19). Overall, the lowest BPc can be found at the deepest stations, with higher values at the shallower stations (Fig. 19). BPc is only correlated with water depth class if the Lander stations are included in the analysis ($r = -0.81$) (Appendix Table 2 & 3). No significant difference in bioturbation potential between sites were detected (t-test, $p = 0.4374$).

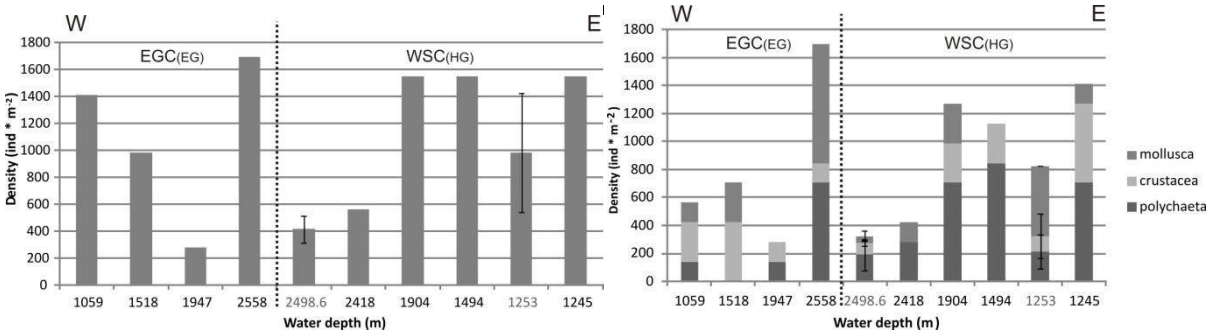

Fig. 16: Mean macrofauna density over the bathymetric gradient and the densities of the 3 most important groups (polychaeta, crustacea and mollusca). The Lander stations are indicated by the error bars and grey water depth labels.

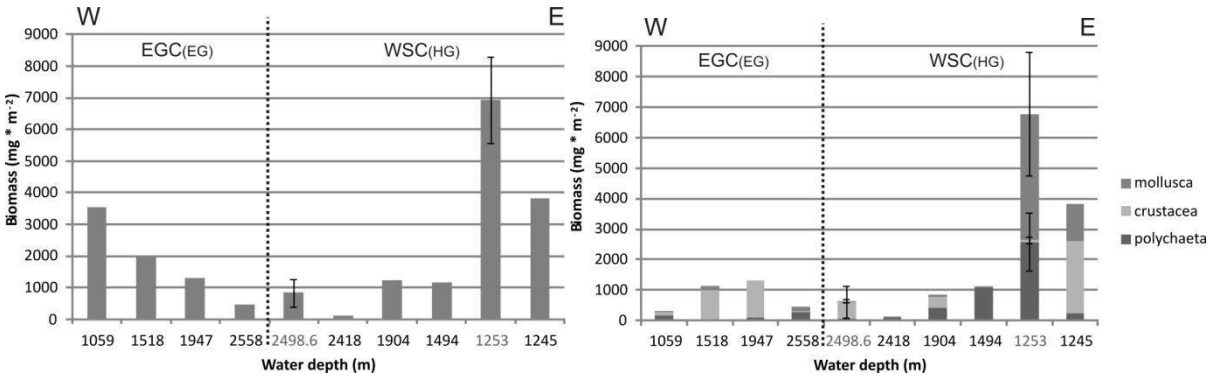

Fig. 17: Mean macrofauna biomass over the bathymetric gradient and the biomass of the 3 most important groups (polychaeta, crustacea and mollusca). The Lander stations are indicated by the error bars and grey water depth labels.

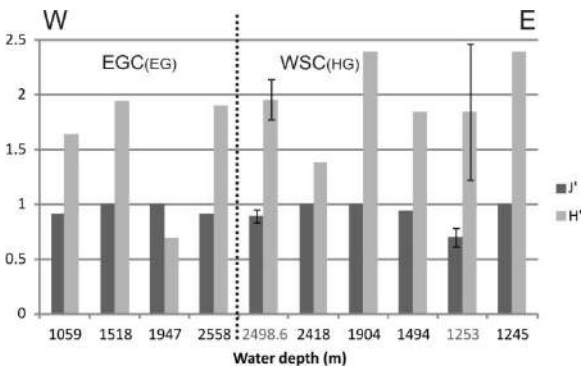

Fig. 18: Pielou's evenness index (J') and Shannon diversity index (H') over the transect. The Lander stations are indicated by the error bars and grey water depth labels.

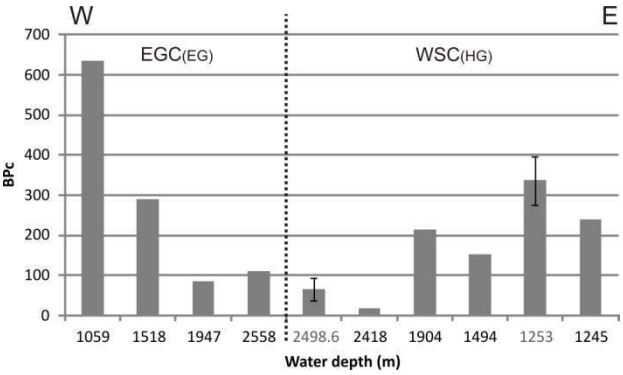

Fig. 19: Community bioturbation potential (BPc) along the transect. The Lander stations are indicated by the error bars and grey water depth labels.

Macrobenthos communities were significantly different between the different water depth classes (ANOSIM R = 0.374 and p = 0.018 for densities and R = 0.509 and p = 0.004 for biomass). The pairwise

test indicated that the greatest difference occurred between 1000 m and 2500 m water depth. Furthermore, communities were also different between the two sites when densities were used (R = 0.47 and p = 0.01; p = 0.144 for biomass). SIMPER analysis found an average dissimilarity of 88.34% between EG and HG sites based on densities. It furthermore indicated that all water depth classes were dissimilar, with values ranging from 72.60% to 90.52% based on densities and 86.04% to 98.55% based on biomass. Moreover based on the densities, SIMPER showed that the polychaete *Myriochele fragilis* was the most important species in EG sites with 30.46%, while in the HG sites *Nematode sp.* contributed most with 36.18%. At 1000 m water depth, the bivalve *Thyasira dunbari* was dominant with 54.56%, while 2500 m water depth was dominated by *Myriochele fragilis* with 38.15%. Based on the biomass, the dominant species at 1000 m water depth was *Thyasira dunbari* with 68.36%, while at 2500 m water depth the dominant species was *Myriochele fragilis* with 66.34%. The Bray-Curtis similarity matrix of the macrofaunal densities and biomass could not significantly be related to the normalized Euclidian distance similarity matrix of the environmental data.

The draftsman correlation plot with log transformed variables, on which the exclusion of correlated variables for the DistLM analysis was based, is shown in Table 8.

The DistLM analysis showed that chlorophyll ($p < 0.04$; AICc = 40.324) significantly explains the variation in macrofaunal density with 38% (the other highly correlated variables, C_{org}, FDA and OM, were also significant but explained less variation and had a higher AICc). Looking at the densities of the three main taxa combined (polychaetes, molluscs and crustaceans), the best model became a combination of FDA and phaeopigment ($p < 0.04$; AICc = 96.268) or FDA and CPE ($p < 0.03$; AIC = 96.274), which explained 45% of the variation. The combination of FDA and phaeopigment ($p < 0.05$; AICc = 97.377) or FDA and CPE ($p < 0.03$; AIC = 97.386) could explain 44% of the variability in polychaete density. Molluscan and crustacean densities could not be analysed separately with DistLM due to their absence in some stations. The same analysis was carried out for the macrofaunal biomass, which was significantly explained for 66% by water depth class ($p < 0.001$; AICc = 47.011). In case of the biomasses of the three main taxa (polychaetes, molluscs and crustaceans), no variable could significantly explain the variation. BPc was explained for 60% by water depth class ($p < 0.003$; AICc = 55.815).

3.2.3. Variation in faunal densities

Up to 76% of the variation in faunal densities (meio- and macrofauna) could be explained by combining chlorophyll ($p < 0.2$) with depth class ($p < 0.05$) and silt ($p \approx 0.2$), with all three variables significant in the sequential test (chlorophyll: $p < 0.3$; depth class: $p < 0.02$; silt $p < 0.05$;

AICc = 19.481). Looking at the most important taxa (nematodes, polychaetes, molluscs and crustaceans), a combination of FDA and phaeopigment ($p < 0.05$; AICc = 95.394) or FDA and CPE ($p < 0.04$; AICc = 95.399) could explain 46% of the variation in the density of the most important taxa.

Unlike the environmental data, no clear patterns can be observed in the PCA plot of the faunal data (Fig. 20). Principle component 1 is correlated with meiofauna density (r = 0.421), nematode density (r = 0.417) and macrofauna density (r = 0.378), and explains 40% of the variation. The second component is correlated with crustacean density (r = 0.329), macrofauna biomass (r = -0.370), polychaeta biomass (r = -0.448) and molluscan biomass (r = -0.4), and explains 25.8%. The differences within the sites seem mainly due to the first component.

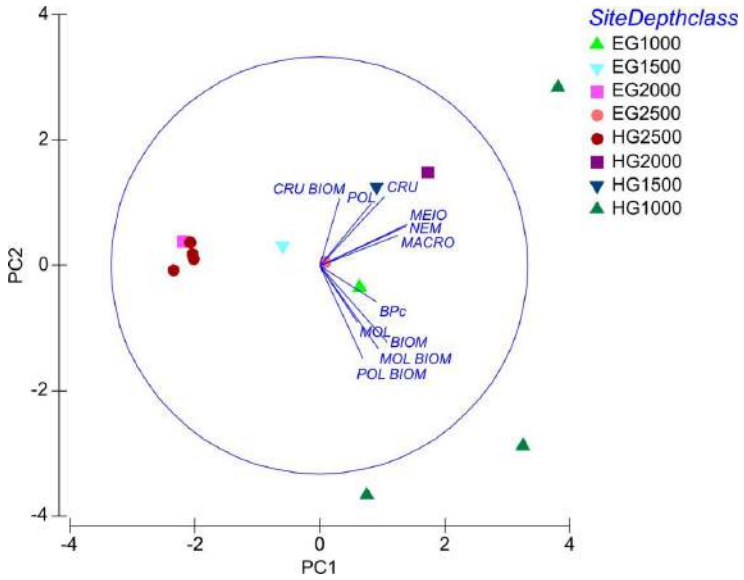

Fig. 20: PCA plot including all faunal variables (MEIO = meiofaunal density, NEM = nematode density, MACRO = macrofaunal density, POL = polychaete density, CRU = crustacean density, MOL = mollusc density, BIOM = macrofaunal biomass, POL BIOM = polychaete biomass, CRU BIOM = crustacean biomass, MOL BIOM = mollusc biomass and BPc = community bioturbation potential). Samples are plotted according to their position in Fram strait (EG-HG) and their water depth (1000 m to 2500 m). PC1 explains 40% of the variation and PC2 25.8%.

Table 5: Macrofaunal densities (individuals/m^2) per taxa for each station. With standard error for the Lander stations.

Station	Depth	Polychaeta	Crustacea	Mollusca	Anthozoa sp.	Nematoda sp.	Nemertea sp.	Sipunculida sp.
MUC_EG I	1059 m	141	282	141	0	0	423	423
MUC_EG II	1518 m	0	423	282	0	0	141	141
MUC_EG III	1947 m	141	141	0	0	0	0	0
MUC_EG IV	2558 m	705	141	846	0	0	0	0
MUC_HG IV	2418 m	282	0	141	0	141	0	0
MUC_HG III	1904 m	705	282	282	0	141	141	0
MUC_HG II	1494 m	846	282	0	0	423	0	0
MUC_HG I	1245 m	705	564	141	0	141	0	0
LANDER_HG IV	2498.6 m	192±112	83±20	50±35	8±10	58±27	25±18	0±0
LANDER_HG I	1253 m	213±124	113±159	500±0	0±0	163±159	0±0	0±0

Table 6: Macrofaunal biomass (mg/m^2) per taxa for each station. With standard error for the Lander stations.

Station	Depth	Polychaeta	Crustacea	Mollusca	Anthozoa sp.	Nematoda sp.	Nemertea sp.	Sipunculida sp.
MUC_EG I	1059 m	173.53	97.34	29.63	0.00	0.00	2662.16	561.50
MUC_EG II	1518 m	0.00	979.09	170.71	0.00	0.00	751.95	69.13
MUC_EG III	1947 m	93.11	1207.64	0.00	0.00	0.00	0.00	0.00
MUC_EG IV	2558 m	292.03	23.98	134.03	0.00	0.00	0.00	0.00
MUC_HG IV	2418 m	77.59	0.00	22.57	0.00	0.00	0.00	0.00
MUC_HG III	1904 m	419.01	355.52	73.36	0.00	1.41	397.84	0.00
MUC_HG II	1494 m	1084.90	38.09	0.00	0.00	26.81	0.00	0.00
MUC_HG I	1245 m	237.01	2372.95	1207.64	0.00	2.82	0.00	0.00
LANDER_HG IV	2498.6 m	76.92±33	517.58±525	52.58±61	107.17±131	1.67±2	80.25±49	0±0
LANDER_HG I	1253 m	2576.50±950	70.13±99	4136.25±2035	0±0	146.13±182	0±0	0±0

3.3. Biogeochemical fluxes

Bio-irrigation is inferred from the influx of bromide into the sediment. The bromide flux along the bathymetrical gradient is represented in Table 7, Fig. 21 and Appendix Fig. 3. The trends in Fig. 21 suggest that bio-irrigation is different according site, as higher fluxes can be found in HG stations. This difference between sites is found to be significant (Kruskal-Wallis test, p = 0.04042).

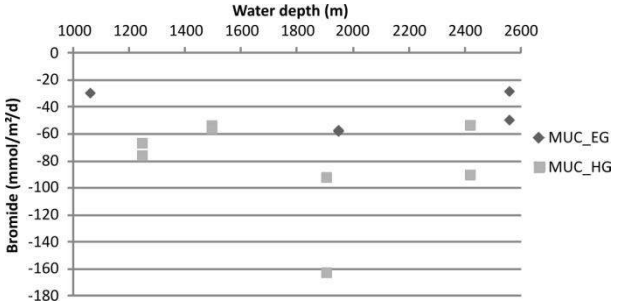

Fig. 21: Bromide flux along the depth gradient, with separation according to site (EG-HG).

Table 7: Biogeochemical variables for each station. Non-significant fluxes are indicated as zero. Bromide fluxes were not measured for the Lander stations and in case a sampling or analysis error was recognised, the flux was not withheld. With Br^- = bromide, O_2 = oxygen, SiO_2 = silicate, PO_4^{3-} = phosphate, NH_4^+ = ammonium, $NO_2^- + NO_3^-$ = nitrite + nitrate, NO_2^- = nitrite.

Station	Core	Depth (m)	Br^- (mmol/m²/d)	O_2 (mmol/m²/d)	SiO_2 (µmol/m²/d)	PO_4^{3-} (µmol/m²/d)	NH_4^+ (µmol/m²/d)	$NO_2^- + NO_3^-$ (µmol/m²/d)	NO_2^- (µmol/m²/d)
MUC_EG I	SC1	1059		1.25	-129	-92	0	-305	
MUC_EG I	SC2	1059	-29	1.41	0	-12	0	0	
MUC_EG II	SC1	1518		1.34	0	-15	0	-226	0
MUC_EG III	SC1	1947	-57	1.25	0	0	-21	0	0
MUC_EG III	SC2	1947	-58	1.59	38	0	-32	0	
MUC_EG4 IV	SC1	2558	-49	1.00	0	0	0	0	
MUC_EG IV	SC2	2558	-28	0.91	0	0	0	0	
MUC_HG IV	SC1	2418	-90	1.59	-132	0	-31	0	0
MUC_HG IV	SC2	2418	-53	1.08	-163	0	-61	0	0
MUC_HG III	SC1	1904	-162	1.42	0	0	0	126	0
MUC_HG III	SC2	1904	-92	0.86	0	0	0	0	-2
MUC_HG II	SC1	1494	-53	0.88	142	0		127	3
MUC_HG II	SC2	1494	-56	0.63	0	0	0	134	3
MUC_HG I	SC1	1245	-76	1.25	178	0		0	0
MUC_HG I	SC2	1245	-66	1.22	0	0		0	0
LANDER_HG IV	K1	2498.6		0.26	0	0		-264	0
LANDER_HG IV	K2	2498.6			-577	-37		-391	-2
LANDER_HG IV	K3	2498.6		0.36	0	0		0	0
LANDER_HG I	K1	1253		1.24	0		0	119	-5
LANDER_HG I	K2	1253			162		0	210	0

Sediment Community Oxygen Consumption (SCOC) or also Total Oxygen Uptake (TOU) is shown in Table 7, Fig. 22 and Appendix Fig. 3. At the shallow HG station, TOU in the *ex situ* measurement (MUC) was very similar to TOU in the *in situ* measurement (LANDER). In the deepest station, TOU *ex situ* measurements (MUC) are higher than the *in situ* measurement (LANDER). No significant differences in TOU were detected between sites (t-test, p = 0.1025).

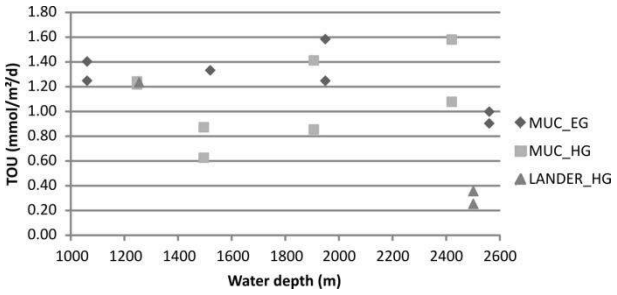

Fig. 22: Total Oxygen Utilization (TOU) along the depth gradient, with separation according to site (EG-HG) and according to sampling method (Lander-MUC).

Nutrient fluxes can be divided in silicate (SiO_2; Table 7 & Fig. 23a), phosphate (PO_4^{3-}; Table 7 & Fig. 23b), ammonium (NH_4^+; Table 7 & Fig. 23c), nitrite + nitrate (NO_2^- + NO_3^-; Table 7 & Fig. 23d) and nitrite (NO_2^-; Table 7 & Fig. 23e) flux (Appendix Fig. 3). Silicate shows an efflux in the shallow HG stations and an influx in the deep HG stations, while it does the opposite in the EG stations (although close to zero flux). For all stations and all water depths, a phosphate and ammonium influx can be observed. Nitrite shows much smaller fluxes than nitrite + nitrate. Both nitrite + nitrate and nitrite show both influx and efflux. Nitrite alone has a small efflux in one shallow *ex situ* HG station, while all the other stations display a small influx. Nitrite + nitrate has an efflux in the shallow and intermediate HG stations (both *in situ* and *ex situ*) and an influx in the shallow EG station and the deep HG station (*in situ*). None of the nutrient fluxes is significantly different between the sites (Kruskal-Wallis test, SiO_2: p-value = 1; PO_4^{3-}: p-value = 0.1201; NH_4^+: p-value = 0.8728; NO_2^- + NO_3^-: p-value = 0.129; NO_2^-: p-value = 0.8397).

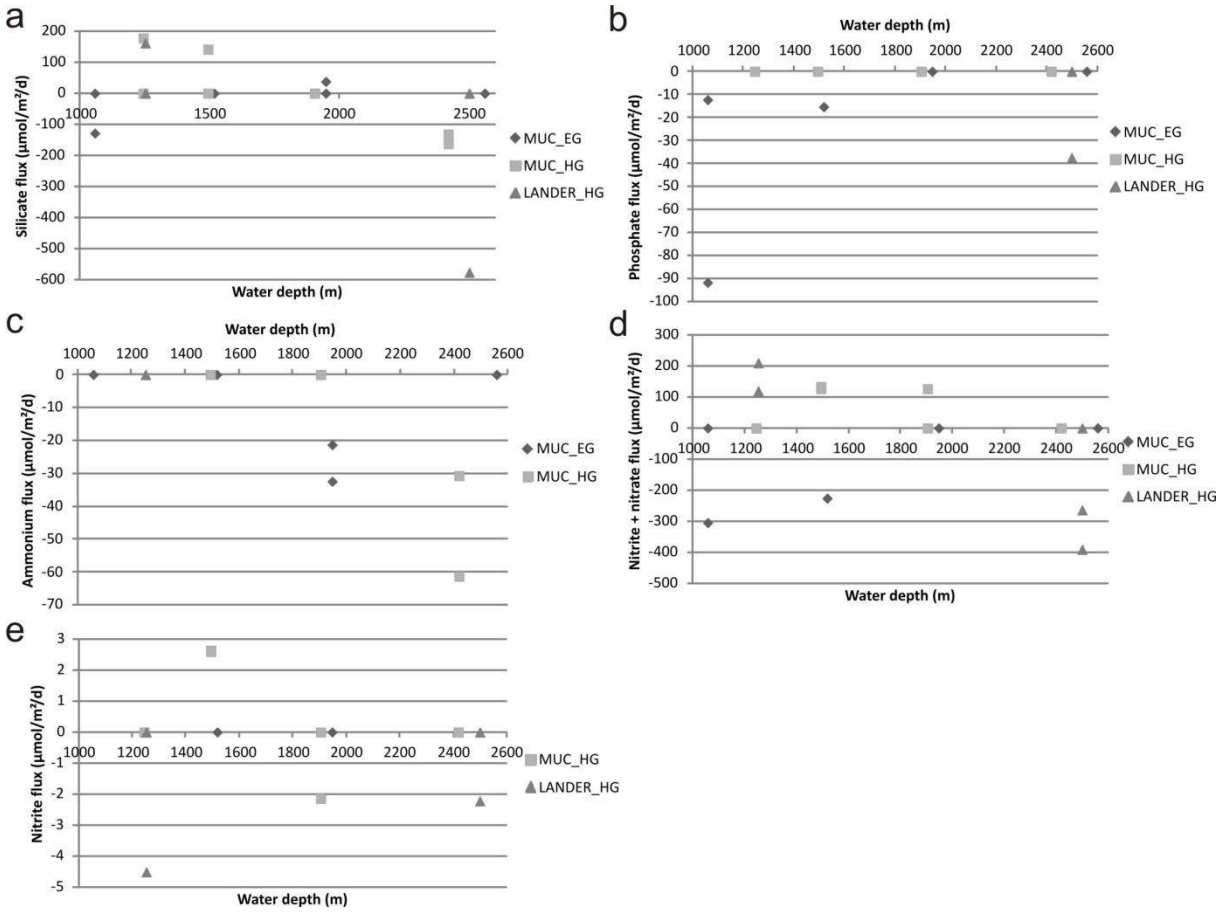

Fig. 23: Nutrient fluxes along the depth gradient: (a) silicate (SiO_2); (b) phosphate (PO_4^{3-}); (c) ammonium (NH_4^+); (d) nitrite + nitrate (NO_2^- + NO_3^-); and (e) nitrite (NO_2^-). With separation according to site (EG-HG) and sampling method (Lander-MUC).

The draftsman correlation matrix shows that phosphate and nitrite + nitrate are correlated to each other (r = 0.87) and that none of the fluxes is correlated to any environmental or faunal variable (Appendix Table 4 & 5).

No clear distribution of the sampling stations can be found according to the biogeochemical fluxes in the PCA plot (Fig. 24). Principle component 1 explains 38.0% of the variation and principle component 2 21.0%. PC1 is correlated with silicate (r = -0.453) and nitrite + nitrate (r = -0.527); PC2 is correlated with oxygen (r = 0.556) and ammonium (r = 0.598).

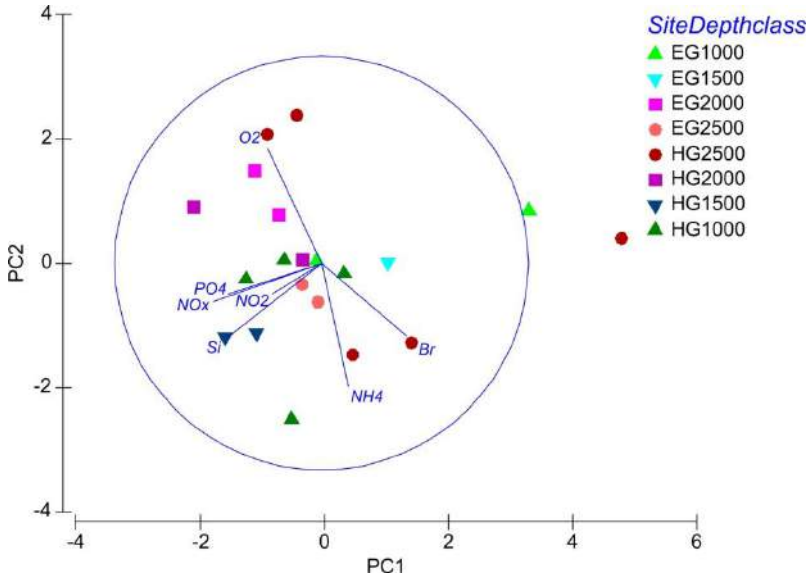

Fig. 24: PCA plot including all biogeochemical variables (Br = bromide, O2 = oxygen, SiO2 = silicate, PO4 = phosphate, NH4 = ammonium, NOx = nitrite + nitrate, NO2 = nitrite). Samples are plotted according to their position in Fram strait (EG-HG) and their water depth (1000 m to 2500 m). PC1 explains 38.0% of the variation and PC2 21.0%.

All above described environmental and faunal variables can be used to try to explain the variation in the biogeochemical flux data with the DistLM analysis. The draftsman correlation plot with log transformed variables, on which the exclusion of correlated variables for the DistLM analysis was based, is shown in Table 8.

The results of this analysis for all fluxes and all stations shows that the best model is explained by only one variable. This is either phaeopigment (AICc = 26.217), CPE (AICc = 26.215), silt (AICc = 26.308), OM (AICc = 26.309), AFDW (AICc = 26.272) or water content (AICc = 26.297) ($p < 0.007$), which are themselves highly correlated. All of them explain around 22% of the variation in all biogeochemical data combined. The other correlated variables, d (0.5), TBN, chlorophyll and C_{org} were also significant but explained less of the variation and had a slightly higher AICc ($\Delta AICc < 1$).

The different fluxes can also be analysed in a separate way. By doing this, TOU can be explained for 60% by silt ($p < 0.005$; AICc = -7.7919). The other correlated variables, TBN, d(0.5), phaeopigment, CPE, OM, AFDW and WC are also significant, but explain less of the variation with a higher AICc. Bromide flux is best explained by OM ($p = 0.039$; AICc = -0.91213), which explains 54% of the variation. Silicate and phosphate fluxes could not be explained by any of the measured environmental or faunal parameters.

Table 8: Transformed draftsman correlation matrix of all environmental and faunal variables: water depth (depth), water depth class (depthclass), median grain size (d (0.5)), silt percentage (silt), chlorophyll a (Chloro), phaeopigments (Phaeo), chloroplastic pigment equivalents (CPE), organic carbon (C.org), ash free dry weight (AFDW), water content (WC), total organic matter (OM), bacterial esterase activity (FDA), total bacterial number (TBN), meiofaunal density (MEIO), nematode density (NEM), macrofaunal density (MACRO), polychaete density (POL), crustacean density (CRU), mollusc density (MOL), macrofaunal biomass (BIOM), polychaete biomass (POL_BIOM), crustacean biomass (CRU_BIOM), mollusc biomass (MOL_BIOM) and community bioturbation potential (BPc). Both data from the MUC and Lander stations was used, after log transformation of most variables. Correlation level of > 0.8 indicated in grey.

	Depth	Depthclas	d	Silt	Chloro	Phaeo	CPE	C.org	AFDW	WC	OM	FDA	TBN	MEIO	NEM	MACRO	POL	CRU	MOL	BIOM	POL_BIOM	CRU_BIOM	MOL_BIOM	BPc
Depth																								
Depthclas	0.989121																							
d	-0.03487	0.032386																						
Silt	-0.24859	-0.15602	0.937162																					
Chloro	-0.20649	-0.15618	0.757861	0.790069																				
Phaeo	-0.21345	-0.13963	0.910696	0.94675	0.943276																			
CPE	-0.21377	-0.13943	0.913678	0.949754	0.94011	0.999949																		
C.org	-0.3144	-0.26148	0.739963	0.819805	0.975447	0.942253	0.939566																	
AFDW	-0.19057	-0.09788	0.960408	0.991252	0.805736	0.953628	0.956419	0.810698																
WC	-0.22934	-0.14121	0.951082	0.998295	0.811719	0.958877	0.961574	0.835636	0.993803															
OM	-0.22688	-0.13312	0.880593	0.928877	0.898791	0.965426	0.965817	0.881894	0.953982	0.936377														
FDA	-0.22061	-0.20664	0.38523	0.428778	0.864758	0.677495	0.670429	0.851588	0.447321	0.458227	0.645386													
TBN	-0.20495	-0.11682	0.961105	0.997044	0.788037	0.947236	0.950326	0.808136	0.995022	0.998573	0.926754	0.418844												
MEIO	-0.55541	-0.57075	0.190617	0.241562	0.650678	0.458642	0.452684	0.619994	0.2632	0.263152	0.460907	0.789831	0.229028											
NEM	-0.53543	-0.55072	0.163664	0.214569	0.64035	0.439107	0.432825	0.607125	0.238359	0.236393	0.445569	0.79855	0.201549	0.998138										
MACRO	-0.52073	-0.51686	0.477442	0.461641	0.623074	0.569498	0.567941	0.581586	0.494679	0.483108	0.58976	0.550183	0.468921	0.729131	0.697305									
POL	-0.02072	-0.0185	0.496268	0.398414	0.769472	0.626875	0.621507	0.710323	0.454532	0.442013	0.607137	0.841834	0.420438	0.626503	0.628154	0.666647								
CRU	-0.21908	-0.18762	0.228936	0.304953	0.26786	0.28493	0.286659	0.330141	0.282316	0.305457	0.286982	0.201925	0.293191	0.187426	0.156233	0.401495	0.317488							
MOL	-0.18465	-0.23852	0.063462	-0.03951	0.047416	0.0054	0.005831	-0.05956	-0.00203	-0.02936	-0.00112	-0.06584	-0.01737	0.330582	0.30723	0.503249	0.017121	-0.17473						
BIOM	-0.81889	-0.85357	-0.30196	-0.15958	-0.1346	-0.18298	-0.18265	-0.04275	-0.20713	-0.17262	-0.17108	-0.00808	-0.19103	0.394506	0.380102	0.301044	-0.11185	0.331162	0.105285					
POL_BIOM	-0.2968	-0.34597	-0.15824	-0.23204	0.090771	-0.06613	-0.0715	0.067149	-0.17916	-0.20528	-0.00298	0.417102	-0.22103	0.561017	0.588877	0.317554	0.470156	-0.22104	0.087838	0.324465				
CRU_BIOM	-0.094	-0.07096	0.04378	0.161689	0.109057	0.11877	0.12074	0.190528	0.109552	0.15076	0.073278	0.043211	0.139122	-0.02098	-0.04013	-0.02511	0.013961	0.839105	-0.34723	0.335119	-0.41206			
MOL_BIOM	-0.44557	-0.53024	-0.16248	-0.20158	-0.01207	-0.12072	-0.12223	-0.05816	-0.2017	-0.1922	-0.18119	0.015766	-0.19577	0.433313	0.415745	0.492935	0.065599	-0.09766	0.820112	0.472838	0.303557	-0.17509		
BPc	-0.82532	-0.82393	0.04032	0.158713	0.09501	0.110757	0.112762	0.15281	0.136782	0.147827	0.166148	0.070132	0.136444	0.419554	0.389871	0.601073	0.071909	0.451017	0.228844	0.874913	0.23857	0.296782	0.469405	

4. Discussion

Both environmental variables and faunal community parameters displayed clear correlations and trends according to water depth and location, as expected and hypothesised. Generally, food availability was higher in the ice-free site and decreased with increasing water depth. This trend in food availability was followed by several faunal community parameters. However the biogeochemical fluxes did not follow any of the expected trends correlated to environmental or faunal variables. In the following part, these general findings will be discussed in more detail.

4.1. Environmental variables

During the sampling campaign in June 2014, the MIZ had just passed above the HG stations (Fig. 25). As the phytoplankton bloom follows the retreating ice edge as it melts, it can be expected that a phytoplankton bloom was formed in the euphotic zone above the HG site at this time (Sakshaug and Skjoldal, 1989). Even despite the high recycling and remineralisation in the upper water column, a relatively high amount organic material can reach the seafloor at the MIZ, up to 50 - 70% of the primary production (in this study 71 - 110 µg/cm^3 OM in the HG stations at 0-1 cm sediment depth) (Bauerfeind et al., 2009; Forest et al., 2010; Jørgensen, 1983; Sakshaug and Skjoldal, 1989; Schlüter et al., 2000; Walsh et al., 1985). The EG stations on the other hand were located in an area with multiyear ice, which remained present at the moment of minimum sea ice extent (Fig. 25 & 26) (Soltwedel et al., 2005). Therefore, organic matter input from the surface after a phytoplankton bloom was limited in the EG stations.

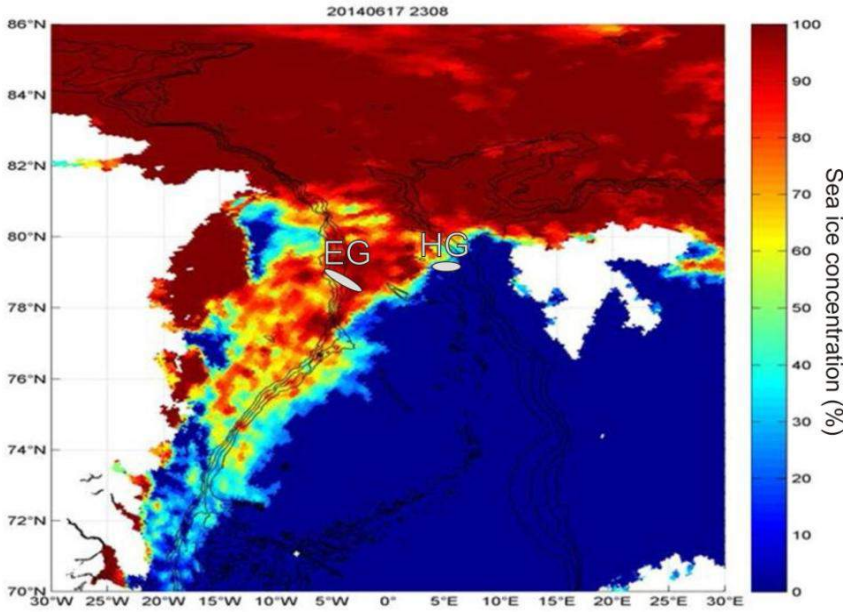

Fig. 25: Sea ice concentration in Fram Strait during the sampling campaign in June 2014, with indication of the MIZ by the light blue colours and indication of the two sampling areas EG and HG. (Drift & Noise Polar Services GmbH, 2014)

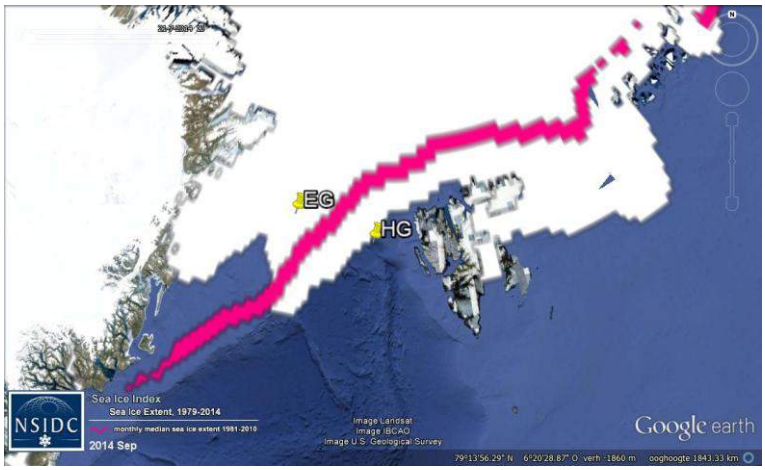

Fig. 26: Minimum sea ice extent in Fram Strait in September 2014, with indication of the sampling areas EG and HG. Pink line = monthly median in sea ice extent in September from 1981 to 2010. (Fetterer et al., 2002)

The EG stations displayed lower pigment, organic carbon and total organic matter content than the HG stations (Table 2 & Fig. 9 & 10). In this study, an C_{org} content of 0.4% to 0.6% was found for the EG stations and 0.7% to 1.5% for the HG stations. This is in agreement with what has been published before by Birgel and Stein (2004) for the whole Fram Strait area. The higher amount of fresh OM, indicated by the higher concentrations of chlorophyll a, in the HG stations could be due to lateral transport by the Atlantic water or to higher input from the surface (Soltwedel et al., 2000). The high share of phaeopigments in the HG stations indicates a high amount of degraded OM and therefore suggests a high input of OM in the past that has been preserved for a long time. In the EG stations, the low OM input was featured by low concentrations of the pigments, even of the degraded phaeopigments. The pigment concentrations were well in agreement with the ones reported by Meyer et al. (2013) for the month July. The trend in food concentration was reflected in the bacterial enzymatic activity (FDA), but not in the bacterial abundance (TBN) (Table 2 & Fig. 11). Therefore it seemed that food input had an influence on microbial life and that with higher food concentrations, the bacterial activity became higher, but not necessarily their densities. Another explanation could be that TBN did not display this trend as bacterial counts were limited to the first sediment cm (as of yet) and no replicates were obtained. In the eastern side of Fram Strait, Soltwedel and Vopel (2001) reported comparable microbial densities, while Soltwedel et al. (2009) reported lower densities, but higher activities. Furthermore, the difference between the two sites was for about 50% explained by differences in organic carbon concentration, pigment concentrations and bacterial activities. Most probably the difference in ice-cover between both sites results in the significant difference between the different variables at the Eastern Greenland and HAUSGARTEN sites. No depth related differences in environmental variables could be found during this study.

Birgel and Stein (2004) reported that the sediments in the western side of Fram Strait are composed of terrigenous inorganic material transported by glaciers. This observation could explain the

occurrence of coarser sediments at the deepest stations (Table 2 & Fig. 7). Therefore, EG stations and mainly the deepest EG station might be under the influence of ice-rafted debris (IRD).

Next to this general trend, station HG III at 1904 m water depth displays an anomalously high peak in OM content, which was also reflected in the pigment concentrations (Fig. 9a & 10). This peak was not detectable in any of the other environmental variables. The uppermost cm of sediment though was displaying similar concentrations of OM and pigments as the other HG stations (Appendix Fig. 1 & 2). Therefore, the reason of this peak has to be sought in the deeper sediment layers. However, the cause of these high concentrations in OM in the deeper layers is unclear. Since hydrographic conditions and direct bioturbation measurements could not be taken into account in this study as of yet (but ^{210}Pb samples for quantification of bioturbation versus accumulation are being processed), their influence cannot be investigated. As a result, at this moment it cannot be ruled out that the peak in OM might be due to high lateral input by the WSC or a specific hydrographic setting (for example a reduced bottom flow (Soltwedel et al., 2013) in the past) or increased bioturbation transporting material to deeper layers. However, the latter was not supported by the BPc index.

4.2. Meiofauna density

Meiofaunal densities obtained during this study were comparable to the densities reported for HAUSGARTEN by Górska et al. (2014) of 300 to 2400 ind. 10 cm^{-2} and lower to the ones reported by Hoste et al. (2007) of 569 to 3303 ind. 10 cm^{-2} at comparable water depths (Table 3 & Fig. 13). A decrease in meiobenthic standing stock with increasing water depth has been observed during this study and confirms previous results of Górska et al. (2014) and Hoste et al. (2007) at the HG site. However, this pattern was not gradual and at mid-water depth (HG III: 1904 m), a peak in meiobenthos density was present. Moreover, this trend with water depth was not statistically significant. However, meiofaunal communities were significantly different according to water depth, but were the same at the two sites. Similarly, meiofaunal density in Górska et al. (2014) and Hoste et al. (2007) was not correlated to water depth, but followed the patterns of OM in the sediment, which were in turn related to water depth. As water depth increases, quantity and quality of the exported matter will decrease due to remineralisation during transport through the water column (Bauerfeind et al., 2009; Forest et al., 2010; Graf, 1989). However, no correlation was found during this study between quantity of food at the seafloor and water depth. Meiofaunal standing stock was found to be structured by food input, indicated by the high correlations found in this study (Appendix Table 3). It has been recognised that the distribution of both density and biomass of benthic organisms is strongly related to the quantity and quality of food supplied to the seabed (Wei *et al.*, 2010). Not only organic matter and chlorophyll concentration, but also bacteria (as indicated by their

enzymatic activity - FDA) was found to be an important food source (this study; Górska et al., 2014; Hoste et al., 2007). Pigment concentrations in the HAUSGARTEN sediments were considerably higher than in other polar regions, due to unusual high fluxes from the surface waters (Górska et al., 2014). This appeared to be even true within the smaller scale of Fram Strait, with much lower concentrations in the western part. As a result, these HG sediments at the MIZ were inhabited by an elevated number of meiofaunal organisms compared to other polar areas (Hoste et al., 2007) and the EG site.

The diversity pattern of decreasing number of meiofauna taxa with increasing water depth observed by Górska et al. (2014), could not be found during this study (Fig. 14). Also the suggested cause of this pattern, food availability, could not be retained as an explanatory variable for the variation in species richness (S). Evenness (J') was for all stations low (maximum: 0.4), mainly due to the fact that 1 taxon, nematodes, was very dominant and made up bulk of the community. EG stations generally showed a higher evenness than HG stations as the nematode abundance was lower, but the species richness the same as in the HG site. Furthermore, it seems that in HAUSGARTEN the meiofauna community became more even towards the shallow stations. The same differentiation between EG and HG and the bathymetric trend in HG could also be found with the Shannon Wiener diversity index (H').

4.3. Macrofauna density and biomass

Macrofauna density in this study is probably underestimated compared to biomass, as all specimen were weighed, but they were not all counted as many of them did not present a head. Therefore it could not be verified if different pieces were one specimen or belonged to several individuals.

Nevertheless, macrofauna densities in HAUSGARTEN (Table 3 & Fig. 16) were comparable to the 300 to 1943 ind. m^{-2} reported by Weslawski et al. (2003) and Wlodarska-Kowalczuk et al. (2004) for the same water depth range. The EG site could not be compared to previous studies in the same area as was the case for the HG site. Therefore a comparison was made to the High Arctic Ocean, which is also permanently ice-covered. Macrofauna densities in the EG site were comparable to those found by Clough et al. (1997) and Kröncke (1998) of 150 to 1575 ind. m^{-2}, but higher than the 5 to 475 ind. m^{-2} found by Paul and Menzies (1974) and Kröncke (1994) in the same water depths.
Macrofauna biomass in HAUSGARTEN is generally lower in this study (Table 3 & Fig. 17) compared to Wlodarska-Kowalczuk et al. (2004) over the same depth range, who found biomasses ranging between 2.2 and 20.9 g ww m^{-2}. These lower biomasses could be due to the difference in sampling

period (June compared to August). In June, the MIZ just broke up which caused the beginning of a phytoplankton bloom and therefore the elevated transport of organic material to the seafloor was starting. In August, the benthic fauna had the time to optimally incorporate this peak in organic matter and gain larger sizes (Wei et al., 2010). Biomass in the EG sites was found to be in accordance with those reported in the permanently ice-covered High Arctic region of 0.09 to 3.44 g ww m^{-2} at water depths of 1000 m to 2500 m (Kröncke, 1998, 1994; Paul and Menzies, 1974). Both benthic abundance and biomass were found to be higher in Fram Strait than in permanently ice-covered areas of the Central Arctic Ocean (Kröncke, 1998; Wlodarska-Kowalczuk et al., 2004). Kröncke (1998) found that benthic species number, density and biomass increased with decreasing distance to Fram Strait. However this is the part of Fram Strait influenced by the WSC and therefore representative for the HG site and not the EG site.

No clear trend in macrofauna density with water depth could be found (Fig. 16). However, macrofauna biomass was found to be correlated and structured by water depth, which was also observed by Wlodarska-Kowalczuk et al. (2004) for the HG site and Kröncke (1998) for the High Arctic. Furthermore, communities in both the HG and EG site differed among water depth. The shallowest stations in both sites were dominated by bivalves, while the deepest were dominated by polychaetes, which is in accordance to what Wlodarska-Kowalczuk et al. (2004) found for the HG site. Moreover, the current study also indicated a strong contrast in communities, according to densities, between ice-covered areas (EG) and ice-free areas (HG) in summer. The ice-covered areas were found to be dominated by polychaetes (deposit feeders), while the ice-free areas were dominated by nematodes (deposit feeders/bacterivorous). Kröncke (1998) also found that permanently ice-covered areas were dominated by deposit feeders in terms of abundance, while Weslawski et al. (2003) found that deposit feeders were dominant in abundance in HAUSGARTEN. No difference in communities could be found between both sites according to biomass. Nor macrofaunal density, nor biomass could be related to the environmental setting.

Wlodarska-Kowalczuk et al. (2004) found a decrease in species richness (S) with water depth, which could not be confirmed by this study (Fig. 18). Furthermore, species richness was comparably high in this study compared to the ones of Wlodarska-Kowalczuk et al. (2004) (8 to 30 per 0.1 m^2) and Kröncke (1998) (1 to 11 per 0.02 m^2). The two diversity indices used, evenness (J') and Shannon (H'), did not show any trend with water depth nor with site. Also Wlodarska-Kowalczuk et al. (2004) was unable to find any water depth related trend in the diversity indices. The high evenness is partly the result of the low number of individuals identified per species, as many specimen did not preserve their head. However, Wlodarska-Kowalczuk et al. (2004) found similar diversities for both indices

(H' between 1.46 and 3.54; J' between 0.54 and 0.93) and noted that diversity might be primarily limited by the available species pool rather than by differences in food availability. This hypothesis could also explain the high similarity between the permanently ice-covered site and the summer ice-free site.

BPc was used to investigate the functional diversity (Braeckman et al., 2014a, 2014b) and appeared to be generally low compared to the highest observed value (Fig. 19). The high value for EG I was due to the high density and biomass of nemerteans and a high density of sipunculids, which are found to have both a high mobility and sediment reworking ability (Queirós et al., 2013). Variability in BPc was correlated to water depth (Table 8 & Appendix Table 2), with lower bioturbation potential towards greater water depths. The absence of nemerteans is the most important reason for the low BPc in the deeper stations. Also cumaceans, which are important bioturbators due to their high biomass, are absent from the deepest stations. Even though sediment reworking species (such as *Lumbrineris sp.*) occur in the deepest stations, they have a low bioturbation potential due to the overall low biomass in these deep areas. Furthermore, *Capitellidae*, due to their high abundance, appear to be important bioturbators in HAUSGARTEN (except for the deepest station). The bivalve *Thyasira dunbari*, due to its high abundance and biomass, is found to be the most important bioturbator in the shallowest HG station.

4.4. Statistical model of relationship between environment and benthic fauna

The best model explaining 76% of the combined variability in density of meio- and macrofauna variation is the model combining water depth with chlorophyll and silt. Further, the best model in explaining the variability in the most important taxa within meio- and macrofauna was bacterial activity combined with phaeopigments or CPE (46%). This indicates that faunal density is dependent on food availability which might be related to water depth (as indicated by Bauerfeind et al. (2009), Forest et al. (2010), and Graf (1989), but not this study). The best model for the combined variation in faunal density (depth + chl a + silt) was also the best model for meiofaunal and nematode density alone and explained even more of the variation (85% and 84%). However, this model was not applicable for the macrofaunal densities. The best model explaining 38% of macrofaunal density was based on chlorophyll alone. This low percentage indicates that other variables influence macrofaunal density as well, for example water depth, however no other variables were found to be significant. That food availability is influencing variation in faunal densities is also indicated by the fact that the best model explaining densities of the three main macrofaunal taxa combined (polychaetes, molluscs and crustaceans) and polychaetes separately is again a combination of bacterial activity and

phaeopigments or CPE (45% and 44%). This difference in best model furthermore indicates that some macrofaunal species are dependent on bacteria as primary food source, while other species have their abundance dependent on other food sources such as freshly deposited algae (chlorophyll a). The fact that bacterial activity and not bacterial number is found to explain density variations could (in part) be due to the fact that bacterial number was (as of yet) only obtained for the first cm of sediment depth and that no replicates were available.

Total macrofaunal biomass could be explained by water depth (66%), although the variability in biomass of the three main taxa combined (polychaetes, molluscs and crustaceans) could not be explained by any environmental variable. This indicates that some species, not belonging to the main taxa, are highly dependent on water depth for their body size.

Bioturbation potential (BPc) was also found to be explained by water depth (60%), indicating that functional diversity is dependent on water depth. In which way water depth was regulating functional diversity is unclear as no other variable is found to explain BPc.

4.5. Biogeochemical cycles

Bio-irrigation, as inferred from the bromide flux, was significantly different in the two sites with higher bio-irrigation in the summer ice-free site (Fig. 21 & Appendix Fig. 3). This indicates that ventilation activity is stronger in this ice-free site and that the overlying seawater is increasingly transported into and within the sediments (Kristensen et al., 2012). Again according to the results found for organic matter and pigment concentration, an increased bio-irrigation rate was observed at HG III at 1904 m water depth. Since the increased concentrations in OM and pigments at this station were found at greater sediment depth (Appendix Fig. 1 & 2), it can be interpreted that this station is characterised by an increased bioturbation rate (both including sediment reworking and burrow ventilation; Kristensen et al., 2012). However, this was not indicated by the bioturbation potential of the present macrofaunal community (BPc; Fig. 19), which is known to have some drawbacks: BPc does not take the effects of bio-irrigation into account (which is a part of bioturbation, Kristensen et al., 2012), it does not include interactions between species, nor interactions between organisms and their abiotic environment (Braeckman et al., 2014a).

Since bio-irrigation is found to exceed molecular diffusion of solutes by as much as an order of magnitude (Kristensen et al., 2012), it was expected that the solute fluxes in this study would also be significantly different between the two sites. However this was not the case for any considered flux. TOU and the nutrient fluxes (SiO_2; PO_4^{3-}; NH_4^+; NO_2^- + NO_3^-; NO_2^-) did not show any statistically significant trend according to water depth nor site (Fig. 22 & 23 & Appendix Fig. 3). This incapability

of finding any trends statistically is most probably due to the high amount of fluxes that were considered insignificant.

The following part contains some hypotheses on how different processes, which were not measured themselves, might influence both sampling sites. Furthermore, due to the high amount of unidentified variation, the many fluxes considered to be insignificant and the low number of replication, it was impossible to verify any of these speculations. To do so, further research is necessary.

The nitrite + nitrate flux showed an influx for the EG and deep stations, while for the shallower HG stations an efflux could be observed. Since these deep sea sediments with low OM supply are highly and deeply oxygenated (Glud, 2008; Sauter et al., 2001), nitrification takes place in which ammonium is oxidized to nitrite and nitrate. The low nitrite fluxes were most likely due to the fact that nitrite is an intermediate product in nitrification (Link et al., 2013a). As nitrite + nitrate showed non-zero fluxes over the whole bathymetric transect, any hypotheses are most easily based on them.

In HAUSGARTEN where bio-irrigation was found to be stronger, nitrate was released from the sediments (Fig. 21 & 23 & Appendix Fig. 3). This indicates that nitrification was very active in the bio-irrigated sites, creating higher nitrate concentrations in the sediments compared to the overlying water and therefore causing a flux from the sediments into the water. It has been reported earlier that the presence of infaunal bioturbators might stimulate the microbial nutrient dynamics (Stief, 2013) and bio-irrigation as well has already been identified as a driver of benthic remineralisation (Davenport et al., 2012; Jørgensen et al., 2005; Na et al., 2008). Furthermore, these sites were located below the spring bloom. Therefore they are characterised by an increased organic matter flux from the surface waters, which causes an increased sediment mineralisation (Jørgensen, 1983; Risgaard-Petersen, 2004). As oxygen is not getting limited by the relatively low OM concentrations at the sediment-water interface, an increased nitrification might be caused and therefore as well an increased denitrification in the deeper anoxic strata (Jørgensen, 1983; Risgaard-Petersen, 2004). As a result, it was expected that due to this high nitrification rates, these stations would be characterised by an ammonium influx (coming from the underlying strata and overlying water) and increased oxygen uptake (coming from the overlying water) (Risgaard-Petersen, 2004). However, only zero fluxes were found for ammonium in these stations and TOU showed no significant differences over the whole transect.

In the Eastern Greenland site on the other hand, bio-irrigation was lower and nitrate could be incorporated into the sediments (Fig. 21 & 23 & Appendix Fig. 3). Since both the EG and HG sites were characterised by the same oxygen concentration in the bottom waters (~300 µmol/L; Table 1), bottom oxygen concentration was not causing this difference in nitrate flux. Therefore a possible explanation could be a reduced, but still active, nitrification in the surface sediments. This nitrate would diffuse to deeper anoxic strata to be subjected to denitrification, forming nitrogen gas (N_2). This downward diffusion could out rate the nitrification and therefore nitrate would need to get incorporated from the overlying water into the sediments. Furthermore, since ammonium was also incorporated into the sediments, it could be interpreted that no other reactions creating ammonium (such as anammox and DNRA; typical for anoxic sediments) were sufficiently present to supply the needed amounts of ammonium for nitrification (Gihring et al., 2010; Jørgensen, 1983; Risgaard-Petersen, 2004).

These hypotheses for both sides of Fram Strait are in agreement with the observed microbial enzymatic activities (FDA; Fig. 11), with low activities at the EG and deep stations and high activities at the shallow HG stations. Furthermore, these hypotheses could also be applied to the measured silicate fluxes, with generally effluxes in the bio-irrigated stations and influxes in the other stations. The same pattern would be expected from the phosphate fluxes, but could not be observed due to the zero fluxes in the shallow HG site. These hypotheses are also in agreement with the observations made by Link et al. (2013a), who found that in deeper waters the benthic activity replenishes the bottom waters with silicate, phosphate and nitrate. Finally, according to these hypotheses, it would be expected that oxygen consumption would be higher in the low bio-irrigation stations as oxygen uptake is the sum of all oxygen consuming processes in the sediment (including diffusive uptake, benthos mediated uptake and oxidation reactions of reduced substances) (Braeckman et al., 2014c; Glud, 2008). However, oxygen showed no such trend and also statistically no differences could be found (Fig. 22 & Appendix Fig. 3).

4.6. Statistical modelling of benthic remineralisation

Half of the variation in the bromide fluxes, indicative of bio-irrigation, could be explained by OM content in the sediment (54%). After the input of fresh OM, benthic activities including bioturbation become higher (Link et al., 2013b; Morata et al., 2013). Furthermore, OM content is to a high extent influenced by bioturbation in terms of sediment reworking, which cannot be decoupled from burrow ventilation or bio-irrigation (Kristensen et al., 2012). It is most likely only a subset of the faunal population that is responsible for the enhanced bioturbation instead of whole communities (or large

taxa) as they were now analysed. TOU was best explained by silt percentage (60%), which is a measure for porosity, thus water content and therefore also oxygen flux (Soltwedel et al., 2013). Silt is also found to be linked to OM content (Clough et al., 1997), on which oxygen consumption is dependent (Jørgensen, 1983; Link et al., 2013a), however in this study no correlation between grain size and OM could be detected. Also TBN explained in a high amount the variability in oxygen consumption (59%). This might be again related to fauna that use bacteria as primary food source. As bacteria themselves also consume oxygen, it can be expected that the higher the bacterial number, the higher the oxygen consumption will be. The nutrient fluxes were never explained by any environmental or faunal variable. This difference between oxygen and nutrient fluxes is most probably the effect of specific species influencing certain fluxes as a response to different nutrient regimes (Link et al., 2013a).

The spatial variation in the different fluxes was not found to be related to faunal community parameters or water depth as indicated by Link et al. (2013b). However, silt fraction was found to explain variations in total oxygen uptake and was moreover correlated to water depth. Also bacterial number, which in fact is a faunal parameter and moreover might determine meiofaunal and macrofaunal community, is found to shape spatial variation in oxygen fluxes. Furthermore, this study could not find the same variables driving the different fluxes as Link et al. (2013a) found for the shallow Canadian Arctic. First of all, this discrepancy might be due to the difference in sampling depth, as this study was conducted in the deep sea (1000 m to 2500 m water depth) and the study by Link et al. (2013a) focussed on the shelf area (< 500 m water depth). Therefore, food availability is highly different, with higher availability in the shallower areas (as already apparent from Fig. 9 & 11) and therefore also higher faunal standing stocks (Fig. 13, 16 & 17). Furthermore, the general trend is an increase in relative importance of fauna-related irrigation for benthic oxygen uptake from the open waters towards the coast (Glud, 2008). This fauna-related oxygen uptake is caused by faunal respiration and activities that expose otherwise anoxic sediments to oxygen (Glud, 2008). Also time of sampling (June versus July/August) might partly explain the difference in driving variables between this study and the one of Link et al. (2013a). As the specific timing determines the regime of food input, the response of the benthic communities as well is different. Next, the nutrient fluxes showed a lot of insignificant fluxes, which makes it harder to explain them. Further, information on faunal community was restricted to a very low sampling effort of 10 sampling stations with only replication for the two Lander stations. Finally, not all driving variables might be included in this study; such as the importance of individual species on specific fluxes, direct bioturbation (not yet available), pH of the sediment pore water and sediment redox conditions (Link et al., 2013a).

5. Conclusion

- A lower food availability was found in the Eastern Greenland site, covered by multiyear ice, than in the HAUSGARTEN site, located underneath the marginal ice zone. Therefore both sites were found to be significantly different from each other in terms of food input. Mainly organic carbon and pigment concentrations and bacterial activity were able to explain the difference between both sites. No correlation was found between food input and water depth, only grain size appeared to be correlated to water depth.

- Meiofaunal densities (137 – 1611 ind. 10 cm^{-2}) were found to be highly related to food availability (chlorophyll a and organic matter concentrations and bacterial activity), but not to water depth. However, meiofaunal communities were significantly different at the different water depths. Communities were the same at both the ice-covered and summer ice-free site. A combination of water depth, chlorophyll a and silt percentage was able to explain 85% of the variability in meiofaunal density.

- Macrofaunal densities (282 – 1693 ind. m^{-2}) had no correlations with any of the environmental variables, while macrofaunal biomass (100 - 3820 mg m^{-2}) was correlated with water depth, as was the macrofaunal community bioturbation potential BPc (18 – 634). Macrofaunal communities were significantly different at the two different sites (EG - HG) in terms of abundance and the different water depths in terms of abundance and biomass. Macrofaunal densities were explained for 38% by chlorophyll a, while density of the three main macrofaunal taxa (polychaetes, molluscs and crustaceans) was explained by a combination of bacterial activity and phaeopigments or CPE (45%). Therefore, macrofaunal densities are most probably influenced by a number of parameters (not necessarily all accounted for in this study) next to food availability. Variations in macrofaunal biomass and BPc were explained by water depth (66% and 60% respectively).

- Bio-irrigation as a part of bioturbation was found to be significantly different between the two sites, with generally higher bio-irrigation rates at the summer ice-free site (HG). For total oxygen uptake and nutrient fluxes, no difference could be found between sites or depths. Bromide flux was explained by organic matter content of the sediments (54%) and total oxygen uptake by silt percentage (60%).

- The proposed hypotheses can be answered as followed:

(1) *meiofaunal and macrofaunal standing stocks decrease with increasing water depth according to decreasing food availability.* No correlation could be found between food availability and water

depth. However, meiofaunal density decreased as food availability decreased and macrofaunal biomass decreased as water depth increased. Macrofaunal density was only partly dependent on food availability.

(2) *faunal communities are significantly different at summer ice-free and ice-covered regions according to food availability.* Food availability is found to be significantly different at the permanently ice-covered site and the summer ice-free site. This difference is reflected in a different macrofaunal community in both sites, but not in a different meiofaunal community.

(3) *food supply and faunal communities explain the variation in benthic remineralisation functioning.* Bio-irrigation was found to be significantly different at the permanently ice-covered site and the summer ice-free site and therefore, organic matter content was able to explain the variation in bromide flux for 54%. Total oxygen uptake was explained for 60% by silt content and for 59% by bacterial number. Bacteria can be seen both as food for higher organisms and as part of the faunal community itself. Therefore, the bigger and more active the bacterial community, the higher the oxygen uptake as benthic remineralisation gets more activated. However the nutrient fluxes could not directly be explained by food availability nor faunal communities.

5.1. Further research

Following the above findings, it is obvious that further research is required. Since the conclusions in this study are based on a very limited data set in terms of replicates, it would be recommended to either redo this study with a higher sampling effort or to continue this study in time with the same sampling effort. In the first case, it would be advisable to have the same number of replication for all investigated variables. Based on the obtained environmental variables in this study, the number of replication should be at least three. Furthermore, some extra variables could be included in the study as indicated in the discussion. These variables could be for instance the specific hydrographic setting, the importance of individual species on specific fluxes, pH and redox conditions in the sediment and nitrification/denitrification rates. In the second case, a time series over at least two years of all variables used during this study should be obtained. To keep the different sampling events comparable within one study, the same sampling stations should be visited and the sampling effort should be the same every time. The first case is highly unlikely to happen due to practicalities in this remote area. The second case however is already planned.

Finally, quantification of bioturbation versus sediment accumulation could not be incorporated in this study as the ^{210}Pb samples were still being processed, but will be included in future studies.

Acknowledgements

First of all I would like to thank Dr. Ulrike Braeckman for giving me the opportunity of doing this thesis and all the guidance and help. It was the first time I did any of this work and I really enjoyed it and learned a lot. Thank you very much for everything! Also, I want to thank Dr. Ellen Pape for the many hours of helping me identifying fauna and Liesbet Colson for checking on the macrofauna. Thanks Guy for the nice time at the meiofauna lab and helping me with any questions I had. Christiane, thank you for sharing an office with me, the nice talks we had and explaining me about statistics and R. Thank you to the whole MARBIOL and Habitat Group for the nice time in Ghent and Bremen.

Furthermore, I want to thank the crew of RV 'Polarstern' and everybody involved in sampling and also the people of AWI deep-sea research group for providing me with extra data on environmental variables. Finally, I would like to thank Katrin Latarius (AWI) for providing us with the map of ice concentration at the moment of sampling.

References

Aargaard, K., Darby, D., Falkner, K., Flato, G., Grebmeier, J., Measures, C., Walsh, J., 1999. Marine Science in the Arctic: A Strategy. Fairbanks, AK.

Anderson, M.J., Gorley, R.N., Clarke, K.R., 2008. PERMANOVA + for PRIMER: guide to software and statistical methods.

Arctic Ocean Map and Bathymetric Chart [WWW Document], n.d. URL http://geology.com/world/arctic-ocean-map.shtml (accessed 5.27.15).

Arrigo, K.R., van Dijken, G., Pabi, S., 2008. Impact of a shrinking Arctic ice cover on marine primary production. Geophys. Res. Lett. 35, 1–6. doi:10.1029/2008GL035028

Bauerfeind, E., Nöthig, E.M., Beszczynska, A., Fahl, K., Kaleschke, L., Kreker, K., Klages, M., Soltwedel, T., Lorenzen, C., Wegner, J., 2009. Particle sedimentation patterns in the eastern Fram Strait during 2000-2005: Results from the Arctic long-term observatory HAUSGARTEN. Deep. Res. Part I Oceanogr. Res. Pap. 56, 1471–1487. doi:10.1016/j.dsr.2009.04.011

Bergmann, M., Soltwedel, T., Klages, M., 2011. The interannual variability of megafaunal assemblages in the Arctic deep sea: Preliminary results from the HAUSGARTEN observatory (79°N). Deep. Res. Part I Oceanogr. Res. Pap. 58, 711–723. doi:10.1016/j.dsr.2011.03.007

Beszczynska-Möller, A., Fahrbach, E., Schauer, U., Hansen, E., 2012. Variability in Atlantic water temperature and transport at the entrance to the Arctic Ocean, 1997-2010. Ices J. Mar. Sci. 69, 852–863. doi:10.1093/icesjms/fst048

Birgel, D., Stein, R., 2004. Northern Fram Strait and Yermak Plateau: distribution, variability and burial of organic carbon and paleoenvironmental implications, in: The Organic Carbon Cycle in the Arctic Ocean. pp. 279–294.

Blicher, M.E., Sejr, M.K., Rysgaard, S., 2009. High carbon demand of dominant macrozoobenthic species indicates their central role in ecosystem carbon flow in a sub-arctic fjord. Mar. Ecol. Prog. Ser. 383, 127–140. doi:10.3354/meps07978

Bodil, B. a., Ambrose, W.G., Bergmann, M., Clough, L.M., Gebruk, A. V., Hasemann, C., Iken, K., Klages, M., MacDonald, I.R., Renaud, P.E., Schewe, I., Soltwedel, T., Włodarska-Kowalczuk, M., 2011. Diversity of the arctic deep-sea benthos. Mar. Biodivers. 41, 87–107. doi:10.1007/s12526-010-0078-4

Boetius, A., Albrecht, S., Bakker, K., Bienhold, C., Felden, J., Fernández-Méndez, M., Hendricks, S., Katlein, C., Lalande, C., Krumpen, T., Nicolaus, M., Peeken, I., Rabe, B., Rogacheva, A., Rybakova, E., Somavilla, R., Wenzhöfer, F., 2013. Export of algal biomass from the melting Arctic sea ice. Science 339, 1430–2. doi:10.1126/science.1231346

Bonaglia, S., Nascimento, F.J. a, Bartoli, M., Klawonn, I., Brüchert, V., 2014. Meiofauna increases bacterial denitrification in marine sediments. Nat. Commun. 5, 5133. doi:10.1038/ncomms6133

Braeckman, U., Foshtomi, M.Y., Van Gansbeke, D., Meysman, F., Soetaert, K., Vincx, M., Vanaverbeke, J., 2014a. Variable Importance of Macrofaunal Functional Biodiversity for Biogeochemical Cycling in Temperate Coastal Sediments. Ecosystems 17, 720–737. doi:10.1007/s10021-014-9755-7

Braeckman, U., Provoost, P., Gribsholt, B., Van Gansbeke, D., Middelburg, J.J., Soetaert, K., Vincx, M., Vanaverbeke, J., 2010. Role of macrofauna functional traits and density in biogeochemical fluxes and bioturbation. Mar. Ecol. Prog. Ser. 399, 173–186. doi:10.3354/meps08336

Braeckman, U., Rabaut, M., Vanaverbeke, J., Degraer, S., Vincx, M., 2014b. Protecting the commons: The use of Subtidal ecosystem engineers in marine management. Aquat. Conserv. Mar. Freshw. Ecosyst. 24, 275–286. doi:10.1002/aqc.2448

Braeckman, U., Van Colen, C., Guilini, K., Van Gansbeke, D., Soetaert, K., Vincx, M., Vanaverbeke, J., 2014c. Empirical Evidence Reveals Seasonally Dependent Reduction in Nitrification in Coastal Sediments Subjected to Near Future Ocean Acidification. PLoS One 9, e108153. doi:10.1371/journal.pone.0108153

Burnham, K.P., Anderson, D.R., 2003. Model selection and multimodel inference: A practical information-theoretic approach, 2nd ed. Springer-Verlag, New York.

Busch, K., Bauerfeind, E., Nöthig, E.-M., 2015. Pteropod sedimentation patterns in different water depths observed with moored sediment traps over a 4-year period at the LTER station HAUSGARTEN in eastern Fram Strait. Polar Biol. 38, 845–859.

Cherkasheva, a., Bracher, a., Melsheimer, C., Köberle, C., Gerdes, R., Nöthig, E.-M., Bauerfeind, E., Boetius, a., 2014. Influence of the physical environment on polar phytoplankton blooms: A case study in the Fram Strait. J. Mar. Syst. 132, 196–207. doi:10.1016/j.jmarsys.2013.11.008

Clarke, K.R., Gorley, R.N., 2006. Primer v6: User manual/Tutorial.

Clough, L.M., Jr., W.G.A., Cochran, K., Barnes, K., P. Renaud, P., Aller, R., 1997. Bioturbation, biomass, and infaunal abundance in the sediments of the Arctic Ocean. Deep Sea Res. Part II. 44, 1683–1704.

Davenport, E.S., Shull, D.H., Devol, A.H., 2012. Roles of sorption and tube-dwelling benthos in the cycling of phosphorus in Bering Sea sediments. Deep. Res. Part II Top. Stud. Oceanogr. 65-70, 163–172. doi:10.1016/j.dsr2.2012.02.004

Doney, S.C., Ruckelshaus, M., Emmett Duffy, J., Barry, J.P., Chan, F., English, C. a., Galindo, H.M., Grebmeier, J.M., Hollowed, A.B., Knowlton, N., Polovina, J., Rabalais, N.N., Sydeman, W.J., Talley, L.D., 2012. Climate Change Impacts on Marine Ecosystems. Ann. Rev. Mar. Sci. 4, 11–37. doi:10.1146/annurev-marine-041911-111611

Drift & Noise Polar Services GmbH, 2014. Drift & Noise [WWW Document]. URL http://driftnoise.com/data-delivery.html (accessed 5.20.15).

Fetterer, F., Knowles, K., Meier, W., Savoie, M., n.d. Sea Ice Index [WWW Document]. Boulder, Color. USA Natl. Snow Ice Data Center. URL http://nsidc.org/data/docs/noaa/g02135_seaice_index/#monthly_extent_image (accessed 5.3.15).

Forest, A., Wassmann, P., Slagstad, D., Bauerfeind, E., Nöthig, E.M., Klages, M., 2010. Relationships between primary production and vertical particle export at the Atlantic-Arctic boundary (Fram Strait, HAUSGARTEN). Polar Biol. 33, 1733–1746. doi:10.1007/s00300-010-0855-3

Gihring, T.M., Lavik, G., Kuypers, M.M.M., Kostka, J.E., 2010. Direct determination of nitrogen cycling rates and pathways in Arctic fjord sediments (Svalbard, Norway). Limnol. Oceanogr. 55, 740–752. doi:10.4319/lo.2009.55.2.0740

Glud, R.N., 2008. Oxygen dynamics of marine sediments. Mar. Biol. Res. 4, 243–289. doi:10.1080/17451000801888726

Glud, R.N., Risgaard-Petersen, N., Thamdrup, B., Fossing, H., Rysgaard, S., 2000. Benthic carbon mineralization in a high-Arctic sound (Young Sound, NE Greenland). Mar. Ecol. Prog. Ser. 206, 59–71. doi:10.3354/meps206059

Górska, B., Grzelak, K., Kotwicki, L., Hasemann, C., Schewe, I., Soltwedel, T., Włodarska-Kowalczuk, M., 2014. Bathymetric variations in vertical distribution patterns of meiofauna in the surface sediments of the deep Arctic ocean (HAUSGARTEN, Fram strait). Deep. Res. Part I Oceanogr. Res. Pap. 91, 36–49. doi:10.1016/j.dsr.2014.05.010

Graf, G., 1989. Benthic-pelagic coupling in a deep-sea benthic community. Nature 341, 437–439. doi:10.1038/341437a0

Heip, C., Vincx, M., Vranken, G., 1985. The ecology of marine nematodes. Ocean. Mar. Biol. Ann. Rev.

Hilligsøe, K.M., Richardson, K., Bendtsen, J., Sørensen, L.L., Nielsen, T.G., Lyngsgaard, M.M., 2011. Linking phytoplankton community size composition with temperature, plankton food web structure and sea-air CO2 flux. Deep. Res. Part I Oceanogr. Res. Pap. 58, 826–838. doi:10.1016/j.dsr.2011.06.004

Hoste, E., Vanhove, S., Schewe, I., Soltwedel, T., Vanreusel, A., 2007. Spatial and temporal variations in deep-sea meiofauna assemblages in the Marginal Ice Zone of the Arctic Ocean. Deep. Res. Part I Oceanogr. Res. Pap. 54, 109–129. doi:10.1016/j.dsr.2006.09.007

Jørgensen, B.B., 1983. Processes at the Sediment-Water interface, in: Bolin, B., Cook, R.B. (Eds.), The Major Biogeochemical Cycles and Their Interactions. SCOPE.

Jørgensen, B.B., Glud, R.N., Holby, O., 2005. Oxygen distribution and bioirrigation in Arctic fjord sediments (Svalbard, Barents Sea). Mar. Ecol. Prog. Ser. 292, 85–95. doi:10.3354/meps292085

Klages, M., Boetius, A., Christensen, J.P., Deubel, H., Piepenburg, D., Schewe, I., Soltwed, 2004. The benthos of Arctic Seas and its role for the organic carbon cycle at the seafloor, in: The Organic Carbon Cycle in the Arctic Ocean. pp. 139–168.

Kristensen, E., Kostka, J.E., 2005. Macrofaunal burrows and irrigation in marine sediment: microbiological and biogeochemical interactions, in: Kristensen, E., Kostka, J.E., Haese, R. (Eds.), Interactions between Macro- and Microorganisms in Marine Sediments. American Geophysical Union, Washington, DC, pp. 125–158. doi:10.1029/CE060p0125

Kristensen, E., Penha-Lopes, G., Delefosse, M., Valdemarsen, T., Quintana, C.O., Banta, G.T., 2012. What is bioturbation? the need for a precise definition for fauna in aquatic sciences. Mar. Ecol. Prog. Ser. 446, 285–302. doi:10.3354/meps09506

Kröncke, I., 1998. Macrofauna communities in the Amundsen Basin, at the Morris Jesup Rise and at the Yermak Plateau (Eurasian Arctic Ocean). Polar Biol. 19, 383–392. doi:10.1007/s003000050263

Kröncke, I., 1994. Macrobenthos composition, abundance and biomass in the Arctic Ocean along a transect between Svalbard and the Makarov Basin. Polar Biol. 14, 519–529. doi:10.1007/BF00238221

Lalande, C., Bauerfeind, E., Nöthig, E.M., Beszczynska-Möller, A., 2013. Impact of a warm anomaly on export fluxes of biogenic matter in the eastern Fram Strait. Prog. Oceanogr. 109, 70–77. doi:10.1016/j.pocean.2012.09.006

Lalande, C., Nöthig, E.-M., Somavilla, R., Bauerfeind, E., Shevchenko, V., Okolodkov, Y., 2014. Variability in under-ice export fluxes of biogenic matter in the Arctic Ocean. Global Biogeochem. Cycles 28, 1–13. doi:10.1002/2013GB004735.Received

Lampitt, R.S., Billett, D.S.M., Rice, a. L., 1986. Biomass of the invertebrate megabenthos from 500 to 4100 m in the northeast Atlantic Ocean. Mar. Biol. 93, 69–81. doi:10.1007/BF00428656

Link, H., Chaillou, G., Forest, A., Piepenburg, D., Archambault, P., 2013a. Multivariate benthic ecosystem functioning in the Arctic-benthic fluxes explained by environmental parameters in the southeastern Beaufort Sea. Biogeosciences 10, 5911–5929. doi:10.5194/bg-10-5911-2013

Link, H., Piepenburg, D., Archambault, P., 2013b. Are Hotspots Always Hotspots? The Relationship between Diversity, Resource and Ecosystem Functions in the Arctic. PLoS One 8, 1–18. doi:10.1371/journal.pone.0074077

Manley, T.O., Bourke, R.H., Hunkins, K.L., 1992. Near-surface circulation over the Yermak plateau in northern Fram Strait. J. Mar. Syst. 3, 107–125. doi:10.1016/0924-7963(92)90033-5

McCartney, M.S., Curry, R.G., Bezdek, H.F., 1996. North Atlantic's transformation pipeline chills and redistributes subtropical water. Oceanus 39, 19–23.

Meyer, K.S., Bergmann, M., Soltwedel, T., 2013. Interannual variation in the epibenthic megafauna at the shallowest station of the HAUSGARTEN observatory (79°N, 6°E). Biogeosciences 10, 3479–3492. doi:10.5194/bg-10-3479-2013

Møller, E.F., Nielsen, T.G., Richardson, K., 2006. The zooplankton community in the Greenland Sea: Composition and role in carbon turnover. Deep Sea Res. Part I Oceanogr. Res. Pap. 53, 76–93. doi:10.1016/j.dsr.2005.09.007

Morán, X.A.G., López-Urrutia, Á., Calvo-Díaz, A., Li, W.K.W., 2010. Increasing importance of small phytoplankton in a warmer ocean. Glob. Chang. Biol. 16, 1137–1144. doi:10.1111/j.1365-2486.2009.01960.x

Morata, N., Michaud, E., Włodarska-Kowalczuk, M., 2013. Impact of early food input on the Arctic benthos activities during the polar night. Polar Biol. 1–16. doi:10.1007/s00300-013-1414-5

Na, T., Gribsholt, B., Galaktionov, O.S., Lee, T., Meysman, F.J.R., 2008. Influence of advective bio-irrigation on carbon and nitrogen cycling in sandy sediments. J. Mar. Res. 66, 691–722.

Nöthig, E.-M., Bauerfeind, E., Beszczynska-Möller, A., Kraft, A., Bracher, A., Cherkasheva, A., Fahl, K., Hardge, K., Kaleschke, L., Lalande, C., Metfies, K., Peeken, I., Klages, M., Soltwedel, T., 2014. Long-term trends in suspended chlorophyll a and vertical particle flux with respect to changing physical conditions in eastern Fram Strait, Arctic Ocean. EGU Gen. Assem. , Vienna, Austria, Geophys. Res. Abstr. 3032, 27 April 2014 - 2 May 2.

Parsons, T.R., Maita, Y., Lalli, C.M., 1984. A Manual of Chemical and Biological Methods for Seawater Analysis. Pergamon Press, Oxford.

Paul, A.Z., Menzies, R.J., 1974. Benthic ecology of the high arctic deep sea. Mar. Biol. 27, 251–262. doi:10.1007/BF00391950

Piechura, J., 2004. The Circulation of the Nordic Seas, in: Skreslet, S. (Ed.), Jan Mayen Island in Scientific Focus. Kluwer Academic Publishers, pp. 91–99.

Piepenburg, D., 2005. Recent research on Arctic benthos: Common notions need to be revised. Polar Biol. 28, 733–755. doi:10.1007/s00300-005-0013-5

Piepenburg, D., Blackburn, T.H., Von Dorrien, C.F., Gutt, J., Hall, P.O.J., Hulth, S., Kendall, M.A., Opalinski, K.W., Rachor, E., Schmid, M.K., 1995. Partitioning of benthic comunity respiration in the Arctic (northwereren Barents Sea). Mar. Ecol. Prog. Ser. 118, 199–213.

Posada, D., Buckley, T.R., 2004. Model selection and model averaging in phylogenetics: advantages of akaike information criterion and bayesian approaches over likelihood ratio tests. Syst. Biol. 53, 793–808. doi:10.1080/10635150490522304

Queirós, A.M., Birchenough, S.N.R., Bremner, J., Godbold, J. a., Parker, R.E., Romero-Ramirez, A., Reiss, H., Solan, M., Somerfield, P.J., Van Colen, C., Van Hoey, G., Widdicombe, S., 2013. A bioturbation classification of European marine infaunal invertebrates. Ecol. Evol. 3, 3958–3985. doi:10.1002/ece3.769

R Core Team, 2015. R: A Language and Environment for Statistical Computing.

Richardson, K., Markager, S., Buch, E., Lassen, M.F., Kristensen, A.S., 2005. Seasonal distribution of primary production, phytoplankton biomass and size distribution in the Greenland Sea. Deep Sea Res. Part I Oceanogr. Res. Pap. 52, 979–999. doi:10.1016/j.dsr.2004.12.005

Risgaard-Petersen, N., 2004. Denitrification, in: Nielsen, S.L., Banta, G.T., Pedersen, M.F. (Eds.), Estuarine Nutrient Cycling: The Influence of Primary Producers. Kluwer Academic Publishers, pp. 263–280.

Sakshaug, E., Skjoldal, H.R., 1989. Life at the Ice Edge. Ambio 18, 60–67.

Sauter, E.J., Schlüter, M., Suess, E., 2001. Organic carbon flux and remineralization in surface sediments from the northern North Atlantic derived from pore-water oxygen microprofiles. Deep. Res. Part I Oceanogr. Res. Pap. 48, 529–553. doi:10.1016/S0967-0637(00)00061-3

Schewe, I., Soltwedel, T., 2003. Benthic response to ice-edge-induced particle flux in the Arctic Ocean. Polar Biol. 26, 610–620. doi:10.1007/s00300-003-0526-8

Schlüter, M., Sauter, E.J., Schäfer, A., Ritzrau, W., 2000. Spatial budget of organic carbon flux to the seafloor of the northern North Atlantic (60°N–80°N). Global Biogeochem. Cycles 14, 329. doi:10.1029/1999GB900043

Smith, W.O., Codispoti, L.A., Nelson, D.M., Manley, T., Buskey, E.J., Niebauer, H.J., Cota, G.F., 1991. Importance of Phaeocystis blooms in the high-latitude ocean carbon cycle. Nature 352, 514–516. doi:10.1038/352514a0

Soltwedel, T., Bauerfeind, E., Bergmann, M., Budaeva, N., Hoste, E., Jaeckisch, N., von Juterzenka, K., Matthiesson, J., Moekievsky, V., Nöthig, E.-M., Quéric, N.-V., Sablotny, B., Sauter, E., Schewe, I., Urban-Malinga, B., Wegner, J., Maria Wlodarska-Kowalczuk, M., Klages, M., 2005. HAUSGARTEN: Multidisciplinary Investigations at a Deep-Sea, Long-Term Observatory in the Arctic Ocean. Oceanography 18, 46–61. doi:10.5670/oceanog.2005.24

Soltwedel, T., Jaeckisch, N., Ritter, N., Hasemann, C., Bergmann, M., Klages, M., 2009. Bathymetric patterns of megafaunal assemblages from the arctic deep-sea observatory HAUSGARTEN. Deep. Res. Part I Oceanogr. Res. Pap. 56, 1856–1872. doi:10.1016/j.dsr.2009.05.012

Soltwedel, T., Mokievsky, V., Rabouille, C., Sauter, E., Volkenandt, M., Hasemann, C., 2013. Effects of experimentally increased near-bottom flow on meiofauna diversity and community structure in the ArcticOcean. Deep. Res. Part I Oceanogr. Res. Pap. 73, 31–45. doi:10.1016/j.dsr.2012.11.008

Soltwedel, T., Mokievsky, V., Schewe, I., 2000. Benthic activity and biomass on the Yermak Plateau and in adjacent deep-sea regions northwest of Svalbard. Deep. Res. Part I Oceanogr. Res. Pap. 47, 1761–1785. doi:10.1016/S0967-0637(00)00006-6

Soltwedel, T., Vopel, K., 2001. Bacterial abundance and biomass in response to organism-generated habitat heterogeneity in deep-sea sediments. Mar. Ecol. Prog. Ser. 219, 291–298. doi:10.3354/meps219291

Spielhagen, R.F., Müller, J., Wagner, A., Werner, K., Lohmann, G., Prange, M., Stein, R., 2015. Holocene variability in the Arctic gateway [WWW Document]. URL http://www.geo.uni-bremen.de/Interdynamik/index.php?option=com_content&task=view&id=35&Itemid=52 (accessed 4.10.15).

Spies, a, Brockmann, U.H., Kattner, G., 1988. Nutrient Regimes in the Marginal Ice-Zone of the Greenland Sea in Summer. Mar. Ecol. Prog. Ser. 47, 195–204. doi:10.3354/meps047195

Stief, P., 2013. Stimulation of microbial nitrogen cycling in aquatic ecosystems by benthic macrofauna: Mechanisms and environmental implications. Biogeosciences 10, 7829–7846. doi:10.5194/bg-10-7829-2013

Van Oevelen, D., Bergmann, M., Soetaert, K., Bauerfeind, E., Hasemann, C., Klages, M., Schewe, I., Soltwedel, T., Budaeva, N.E., 2011. Carbon flows in the benthic food web at the deep-sea observatory HAUSGARTEN (Fram Strait). Deep. Res. Part I Oceanogr. Res. Pap. 58, 1069–1083. doi:10.1016/j.dsr.2011.08.002

Walsh, J.E., 2008. Climate of the Arctic marine environment. Ecol. Appl. 18, S3–S22. doi:10.1890/06-0503.1

Walsh, J.J., McRoy, C.P., Blackburn, T.H., Coachman, L.K., Goering, J.J., Nihoul, J.J., Parker, P.L., Springer, A.M., Tripp, R.B., Whitledge, T.E., Wirick, C.D., 1985. The role of Bering Strait in the Carbon/Nitrogen Fluxes of Polar Marine Ecosystems, in: Rey, L., Alexander, V. (Eds.), Marine Living Systems in the Far North. E.J. Brill, Leiden, pp. 90–120.

Wassmann, P., Slagstad, D., Ellingsen, I., 2010. Primary production and climatic variability in the European sector of the Arctic Ocean prior to 2007: Preliminary results. Polar Biol. 33, 1641–1650. doi:10.1007/s00300-010-0839-3

Wei, C.-L., Rowe, G.T., Escobar-Briones, E., Boetius, A., Soltwedel, T., Caley, M.J., Soliman, Y., Huettmann, F., Qu, F., Yu, Z., Pitcher, C.R., Haedrich, R.L., Wicksten, M.K., Rex, M. a, Baguley, J.G., Sharma, J., Danovaro, R., MacDonald, I.R., Nunnally, C.C., Deming, J.W., Montagna, P., Lévesque, M., Weslawski, J.M., Wlodarska-Kowalczuk, M., Ingole, B.S., Bett, B.J., Billett, D.S.M., Yool, A., Bluhm, B. a, Iken, K., Narayanaswamy, B.E., 2010. Global patterns and predictions of seafloor biomass using random forests. PLoS One 5, e15323. doi:10.1371/journal.pone.0015323

Weslawski, J., Wlodarska-Kowalczuk, M., Legezynska, J., 2003. Occurrence of soft bottom macrofauna along the depth gradient in High Arctic, 79 N. Pol. Polar Res 24, 73–88.

Wlodarska-Kowalczuk, M., Kendall, M. a., Marcin Weslawski, J., Klages, M., Soltwedel, T., 2004. Depth gradients of benthic standing stock and diversity on the continental margin at a high-latitude ice-free site (off Spitsbergen, 79°N). Deep. Res. Part I Oceanogr. Res. Pap. 51, 1903–1914. doi:10.1016/j.dsr.2004.07.013

Appendix

Table 1: Draftsman correlation matrix with the environmental variables: water depth (depth), median grain size (d (0.5)), silt percentage (silt), chlorophyll a (Chloro. A), phaeopigments (Phaeo. A), chloroplastic pigment equivalents (CPE), organic carbon (C-org), ash free dry weight (AFDW), water content (WC), total organic matter (OM), bacterial esterase activity (FDA), bacterial biomass (BBM) and total bacterial number (TBN). Only data from the MUC was available for the environmental variables. Correlation level of > 0.8 indicated in grey.

	Depthclass	d (0.5)	Silt	Chloro. A	Phaeo. A	CPE	C-org	AFDW	WC	OM	FDA	TBN
Depthclass	/											
d (0.5)	0.6303779	/										
Silt	-0.829853	-0.95029	/									
Chloro. A	-0.321655	-0.17419	0.236351	/								
Phaeo. A	-0.321149	-0.18363	0.248969	0.996237	/							
CPE	-0.32132	-0.18268	0.247699	0.997004	0.999956	/						
C-org	-0.415085	-0.26086	0.350215	0.964312	0.980801	0.979378	/					
AFDW	0.2095428	0.00414	-0.08981	0.251708	0.219218	0.222801	0.166195	/				
WC	-0.676441	-0.52674	0.648855	0.824583	0.849687	0.847287	0.923238	0.038297	/			
OM	-0.043954	-0.18046	0.1475	0.548294	0.531546	0.533545	0.514673	0.918929	0.424519	/		
FDA	-0.370481	-0.19646	0.289627	0.955063	0.972337	0.970827	0.993745	0.220785	0.904313	0.561058	/	
TBN	-0.706208	-0.14969	0.404896	0.496335	0.52759	0.52441	0.634134	-0.30277	0.765991	0.033794	0.641729	/

Table 2: Draftsman correlation matrix with the faunal variables: water depth (depth), meiofaunal density (MEIO), nematode density (NEM), macrofaunal density (MACRO), polychaete density (POL), crustacean density (CRU), mollusc density (MOL), macrofaunal biomass (BIOM), polychaete biomass (POL BIOM), crustacean biomass (CRU BIOM), mollusc biomass (MOL BIOM) and community bioturbation potential (BPc). Both data from the MUC and Lander were available and used. Correlation level of > 0.8 indicated in grey.

	Depthclass	MEIO	NEM	MACRO	POL	CRU	MOL	BIOM	POL BIOM	CRU BIOM	MOL BIOM	BPc
Depthclass	/											
MEIO	-0.539119	/										
NEM	-0.525932	0.99837	/									
MACRO	-0.461615	0.668066	0.659327	/								
POL	-0.018502	0.638148	0.645494	0.733358	/							
CRU	-0.551448	0.65515	0.627015	0.63718	0.365535	/						
MOL	-0.139947	0.085125	0.08047	0.462716	0.178645	-0.06828	/					
BIOM	-0.820576	0.408411	0.401686	0.2243	-0.16139	0.199864	0.343839	/				
POL BIOM	-0.563806	0.188135	0.208025	0.10167	-0.00585	-0.22702	0.426287	0.739558	/			
CRU BIOM	-0.174712	0.372228	0.342967	-0.04298	0.012991	0.608509	-0.324	0.054386	-0.32705	/		
MOL BIOM	-0.576858	0.351238	0.351387	0.156923	-0.07518	0.019824	0.443233	0.906741	0.7283949	-0.094548	/	
BPc	-0.808266	0.285136	0.269951	0.480944	-0.14612	0.43948	0.200241	0.667947	0.3006018	-0.037403	0.3818031	/

Table 3: Draftsman correlation matrix with the environmental and faunal variables: water depth (depth), median grain size (d (0.5)), silt percentage (silt), chlorophyll a (Chloro. A), phaeopigments (Phaeo. A), chloroplastic pigment equivalents (CPE), organic carbon (C-org), ash free dry weight (AFDW), water content (WC), total organic matter (OM), bacterial esterase activity (FDA), total bacterial number (TBN), meiofaunal density (MEIO), nematode density (NEM), macrofaunal density (MACRO), polychaete density (POL), crustacean density (CRU), mollusc density (MOL), macrofaunal biomass (BIOM), polychaete biomass (POL BIOM), crustacean biomass (CRU BIOM), mollusc biomass (MOL BIOM) and community bioturbation potential (BPc). Since the environmental variables had only data from the MUC, only the MUC station were retained. Correlation level of > 0.8 indicated in grey.

	Depthclass	d (0.5)	Silt	Chloro. A	Phaeo. A	CPE	C-org	AFDW	WC	OM	FDA	TBN	MEIO	NEM	MACRO	POL	CRU	MOL	BIOM	POL BIOM	CRU BIOM	MOL BIOM	BPc
Depthclass	/																						
d (0.5)	0.63037795	/																					
Silt	-0.8298526	-0.95029	/																				
Chloro. A	-0.32165467	-0.17419	0.236351	/																			
Phaeo. A	-0.32114891	-0.18363	0.248969	0.996237	/																		
CPE	-0.32131975	-0.18268	0.247699	0.997004	0.999956	/																	
C-org	-0.41508492	-0.26086	0.350215	0.964312	0.980801	0.979378	/																
AFDW	0.209542766	0.00414	-0.08981	0.251708	0.219218	0.222801	0.166195	/															
WC	-0.67644108	-0.52674	0.648855	0.824583	0.849687	0.847287	0.923238	0.038297	/														
OM	-0.04395386	-0.18046	0.1475	0.548294	0.531546	0.533545	0.514673	0.918929	0.424519	/													
FDA	-0.37048147	-0.19646	0.289627	0.955063	0.972337	0.970827	0.993745	0.220785	0.904313	0.561058	/												
TBN	-0.70620832	-0.14969	0.404896	0.496335	0.52759	0.52441	0.634134	-0.30277	0.765991	0.033794	0.641729	/											
MEIO	-0.44750714	-0.22093	0.309689	0.974986	0.960688	0.962578	0.932684	0.308597	0.822713	0.589032	0.922372	0.511635	/										
NEM	-0.41885841	-0.22758	0.304213	0.975928	0.961688	0.963572	0.932732	0.357239	0.818353	0.632882	0.925764	0.484847	0.998118	/									
MACRO	-0.31943828	0.308558	-0.07805	0.507886	0.493683	0.495394	0.492431	0.38977	0.412771	0.510745	0.54186	0.567099	0.580478	0.575457	/								
POL	0.076077469	0.350654	-0.26228	0.719987	0.731843	0.73083	0.723207	0.41928	0.516566	0.610595	0.790676	0.470512	0.665764	0.681879	0.70476	/							
CRU	-0.81508761	-0.38668	0.574541	0.565708	0.54265	0.545333	0.545201	-0.16456	0.67071	0.089884	0.502611	0.691619	0.63611	0.606969	0.474793	0.151985	/						
MOL	0.466252404	0.905949	-0.82573	-0.14685	-0.18035	-0.1768	-0.29091	0.094102	-0.52682	-0.11747	-0.24582	-0.17904	-0.14621	-0.15741	0.446817	0.232534	-0.14158	/					
BIOM	-0.9302797	-0.48899	0.676315	0.340581	0.319977	0.322315	0.365438	-0.23461	0.544272	-0.04238	0.310299	0.566105	0.491036	0.453331	0.299007	-0.12939	0.796551	-0.30133	/				
POL BIOM	-0.12053107	-0.01273	0.106453	0.375491	0.418073	0.413632	0.518692	0.356346	0.548852	0.57579	0.59274	0.575925	0.331085	0.357823	0.518179	0.745821	0.076722	-0.16905	-0.14863	/			
CRU BIOM	-0.48193607	-0.32576	0.366191	0.497239	0.47601	0.478471	0.43503	-0.47845	0.4589	-0.27042	0.366987	0.380503	0.496489	0.462102	-0.09844	-0.04047	0.697699	-0.26135	0.605153	-0.304349	/		
MOL BIOM	-0.48669804	-0.10242	0.230793	0.753834	0.741821	0.743385	0.700804	-0.33153	0.622151	-0.07654	0.647127	0.541984	0.754572	0.716898	0.312713	0.300318	0.729982	-0.01985	0.629308	-0.124984	0.8379688	/	
BPc	-0.74809577	-0.35609	0.533636	-0.11338	-0.13828	-0.13565	-0.07559	0.068188	0.148267	0.074189	-0.09835	0.266131	0.090346	0.069345	0.356222	-0.309	0.455477	-0.10725	0.764494	-0.121004	-0.0046329	0.0557333	/

Table 4: Draftsman correlation matrix with the environmental and biogeochemical variables: water depth (depth), median grain size (d (0.5)), silt percentage (silt), chlorophyll a (Chloro. A), phaeopigments (Phaeo. A), chloroplastic pigment equivalents (CPE), organic carbon (C-org), ash free dry weight (AFDW), water content (WC), total organic matter (OM), bacterial esterase activity (FDA), total bacterial number (TBN), total oxygen utilization (O_2), bromide (Br), silicate (Si), phosphate (PO_4), Ammonium (NH_4), nitrite + nitrate ($NO_2 + NO_3$) and nitrite (NO_2). Since the environmental variables had only data from the MUC, only the MUC station were retained. Correlation level of > 0.8 indicated in grey.

	Depthclass	d (0.5)	Silt	Chloro. A	Phaeo. A	CPE	C-org	AFDW	WC	OM	FDA	TBN	O_2	Br	Si	PO_4	NH_4	NO_x	NO_2
Depthclass	/																		
d (0.5)	0.6303779	/																	
Silt	-0.8298526	-0.95029	/																
Chloro. A	-0.3216547	-0.17419	0.236351	/															
Phaeo. A	-0.3211489	-0.18363	0.248969	0.996237	/														
CPE	-0.3213197	-0.18268	0.247699	0.997004	0.999956	/													
C-org	-0.4150849	-0.26086	0.350215	0.964312	0.980801	0.979378	/												
AFDW	0.2095428	0.00414	-0.08981	0.251708	0.219218	0.222801	0.166195	/											
WC	-0.6764411	-0.52674	0.648855	0.824583	0.849687	0.847287	0.923238	0.038297	/										
OM	-0.0439539	-0.18046	0.1475	0.548294	0.531546	0.533545	0.514673	0.918929	0.424519	/									
FDA	-0.3704815	-0.19646	0.289627	0.955063	0.972337	0.970827	0.993745	0.220785	0.904313	0.561058	/								
TBN	-0.7062083	-0.14969	0.404896	0.496335	0.52759	0.52441	0.634134	-0.30277	0.765991	0.033794	0.641729	/							
O_2	-0.0944437	-0.39947	0.266018	-0.31418	-0.34711	-0.34368	-0.39888	-0.30258	-0.32223	-0.44075	-0.48533	-0.51545	/						
Br	-0.4457066	-0.01487	0.199861	-0.58371	-0.58847	-0.58817	-0.51936	-0.42485	-0.25751	-0.50508	-0.53289	0.234063	0.13274	/					
Si	-0.3644715	-0.07484	0.190248	0.635045	0.646093	0.645135	0.667957	-0.20049	0.67806	0.109024	0.681202	0.764436	-0.46314	-0.18115	/				
PO_4	0.4166055	0.302951	-0.38557	0.439573	0.44119	0.441175	0.366016	0.041697	0.163373	0.144673	0.400251	0.102977	-0.40834	-0.61552	0.670744	/			
NH_4	-0.5590328	0.084622	0.157354	0.285464	0.255447	0.258777	0.26474	0.179676	0.34319	0.288046	0.296483	0.627801	-0.46025	0.452311	0.46308	-0.02931	/		
NO_x	0.4064931	0.106088	-0.21803	0.425172	0.433838	0.433061	0.376367	0.278389	0.226543	0.384223	0.412446	0.030916	-0.49635	-0.6295	0.54523	0.900456	-0.02669	/	
NO_2	-0.2227791	-0.07023	0.204071	-0.07257	0.005442	-0.00297	0.168652	-0.48126	0.3442	-0.26735	0.18858	0.632519	-0.50355	0.242437	0.360451	0.029997	0.027425	0.060528	/

Table 5: Draftsman correlation matrix with the faunal and biogeochemical variables: meiofaunal density (MEIO), nematode density (NEM), macrofaunal density (MACRO), polychaete density (POL), crustacean density (CRU), mollusc density (MOL), macrofaunal biomass (BIOM), polychaete biomass (POL BIOM), crustacean biomass (CRU BIOM), mollusc biomass (MOL BIOM) and community bioturbation potential (BPc), total oxygen utilization (O_2), bromide (Br), silicate (Si), phosphate (PO_4), Ammonium (NH_4), nitrite + nitrate (NO_2 + NO_3) and nitrite (NO_2). Both data from the MUC and Lander were available and used (except for bromide). Correlation level of > 0.8 indicated in grey.

	MEIO	NEM	MACRO	POL	CRU	MOL	BIOM	POL BIOM	CRU BIOM	MOL BIOM	BPc	O_2	Br	Si	PO_4	NH_4	NO_x	NO_2
MEIO																		
NEM	0.99837																	
MACRO	0.668066	0.659327																
POL	0.638148	0.645494	0.733358															
CRU	0.65515	0.627015	0.63718	0.365535														
MOL	0.085125	0.08047	0.462716	0.178645	-0.06828													
BIOM	0.408411	0.401686	0.2243	-0.16139	0.199864	0.343839												
POL BIOM	0.188135	0.208025	0.10167	-0.00585	-0.22702	0.426287	0.739558											
CRU BIOM	0.372228	0.342967	-0.04298	0.012991	0.608509	-0.324	0.054386	-0.32705										
MOL BIOM	0.351238	0.351387	0.156923	-0.07518	0.019824	0.443233	0.906741	0.728395	-0.094548									
BPc	0.285136	0.269951	0.480944	-0.14612	0.43948	0.200241	0.667947	0.300602	-0.037403	0.3818031								
O_2	0.307768	0.290078	0.433263	0.159057	0.526703	0.072421	0.042929	-0.328827	0.178288	0.0143269	0.317198							
Br	-0.47639	-0.4914	-0.2974	-0.62264	-0.19447	0.098439	0.355794	0.237372	-0.189881	0.2893656	0.328496	-0.49369						
Si	0.439376	0.434174	0.46658	0.47605	0.409533	0.179542	0.128392	0.204116	-0.045305	0.1638663	0.06408	0.376633	-0.29865					
PO_4	0.362652	0.377793	0.176783	0.428172	0.038529	0.346319	0.092872	0.355946	0.001627	0.3055951	-0.40367	0.089424	-0.4042	0.658347				
NH_4	0.24833	0.241295	0.414244	0.173051	0.377416	0.237838	0.316543	0.227886	0.043235	0.1984087	0.392444	-0.3911	0.534032	0.094758	-0.04183			
NO_x	0.393498	0.415595	0.308637	0.331512	0.061301	0.418327	0.298541	0.581808	-0.209828	0.4154543	-0.06055	0.207589	-0.37163	0.671369	0.872418	-0.06761		
NO_2	-0.18559	-0.19164	0.034558	0.223179	0.043032	-0.28067	-0.50929	-0.156096	-0.073034	-0.621834	-0.21557	-0.05412	-0.18643	0.382723	0.040274	-0.12257	0.060253	

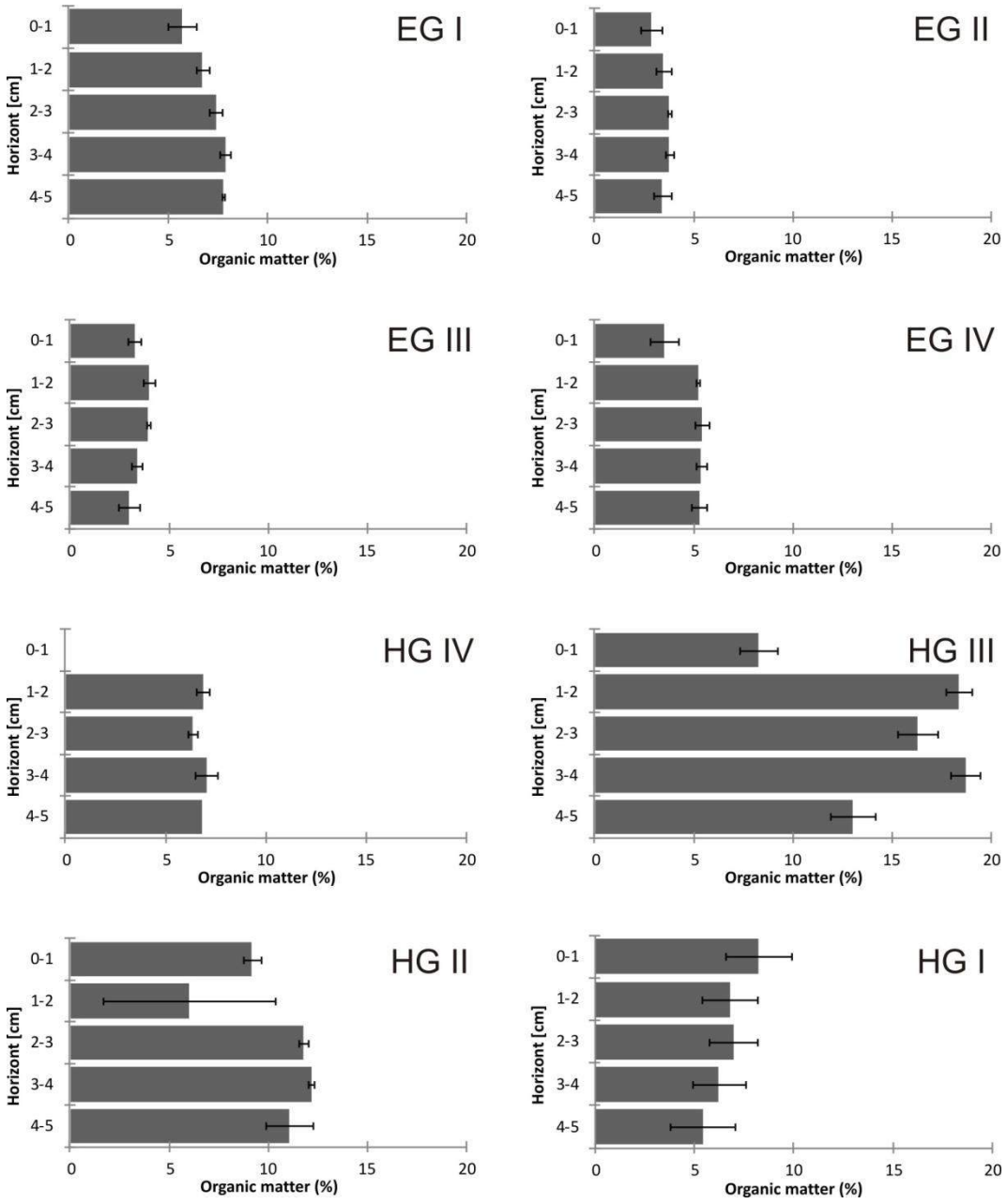

Fig. 1: Organic matter content (%) over the 5 cm sediment depth for each sampling station. Station HG IV had a measurement error at depth interval 0-1 cm and is therefore not represented. Station HG III shows the anomalously high organic matter content at the deeper layers.

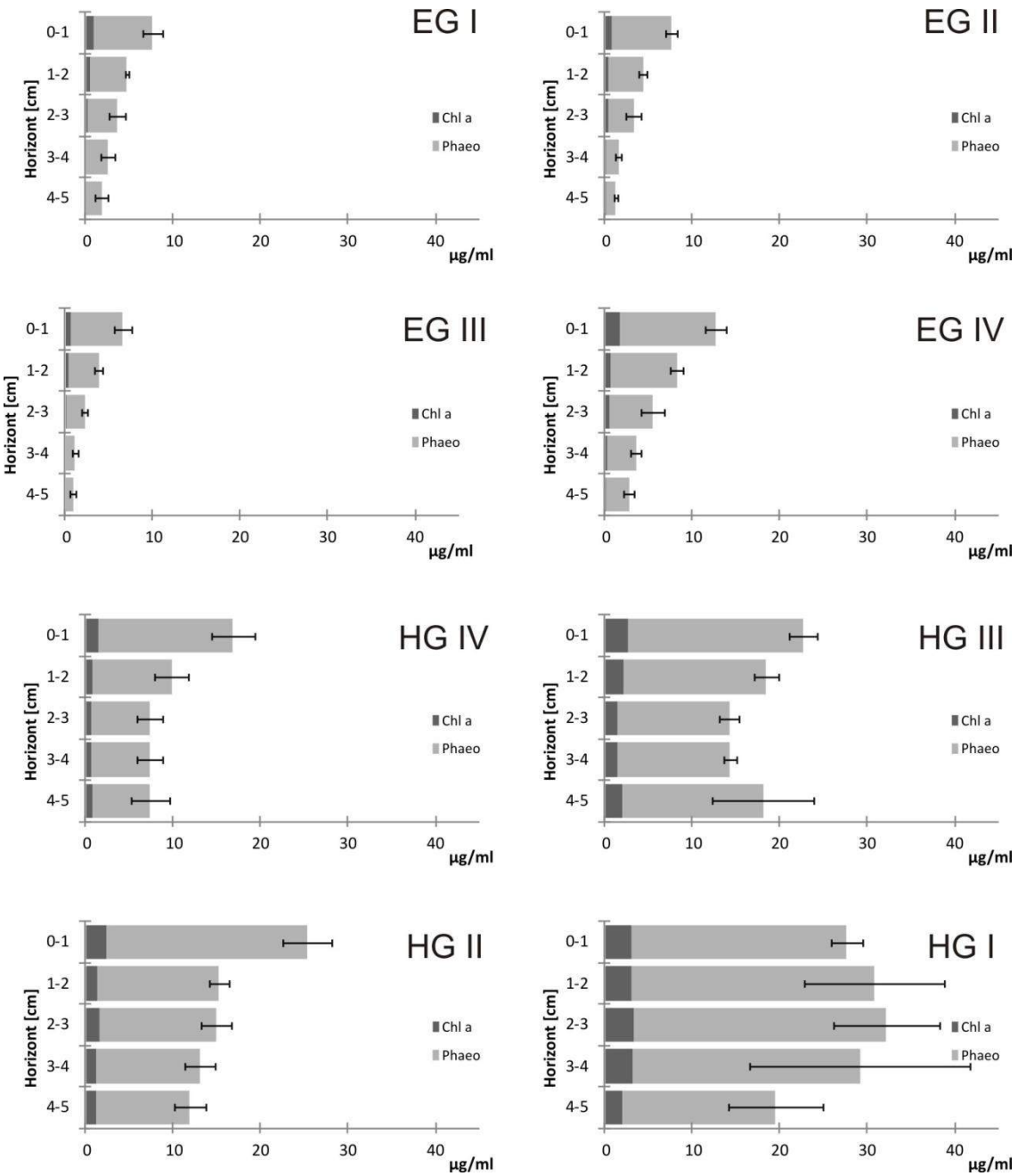

Fig. 2: Pigment concentration (µg/mL) of both chlorophyll a (chl a) and phaeopigments over the 5 cm sediment depth for each sampling station. Stations HG III shows the increase in pigment concentration at the deepest layer.

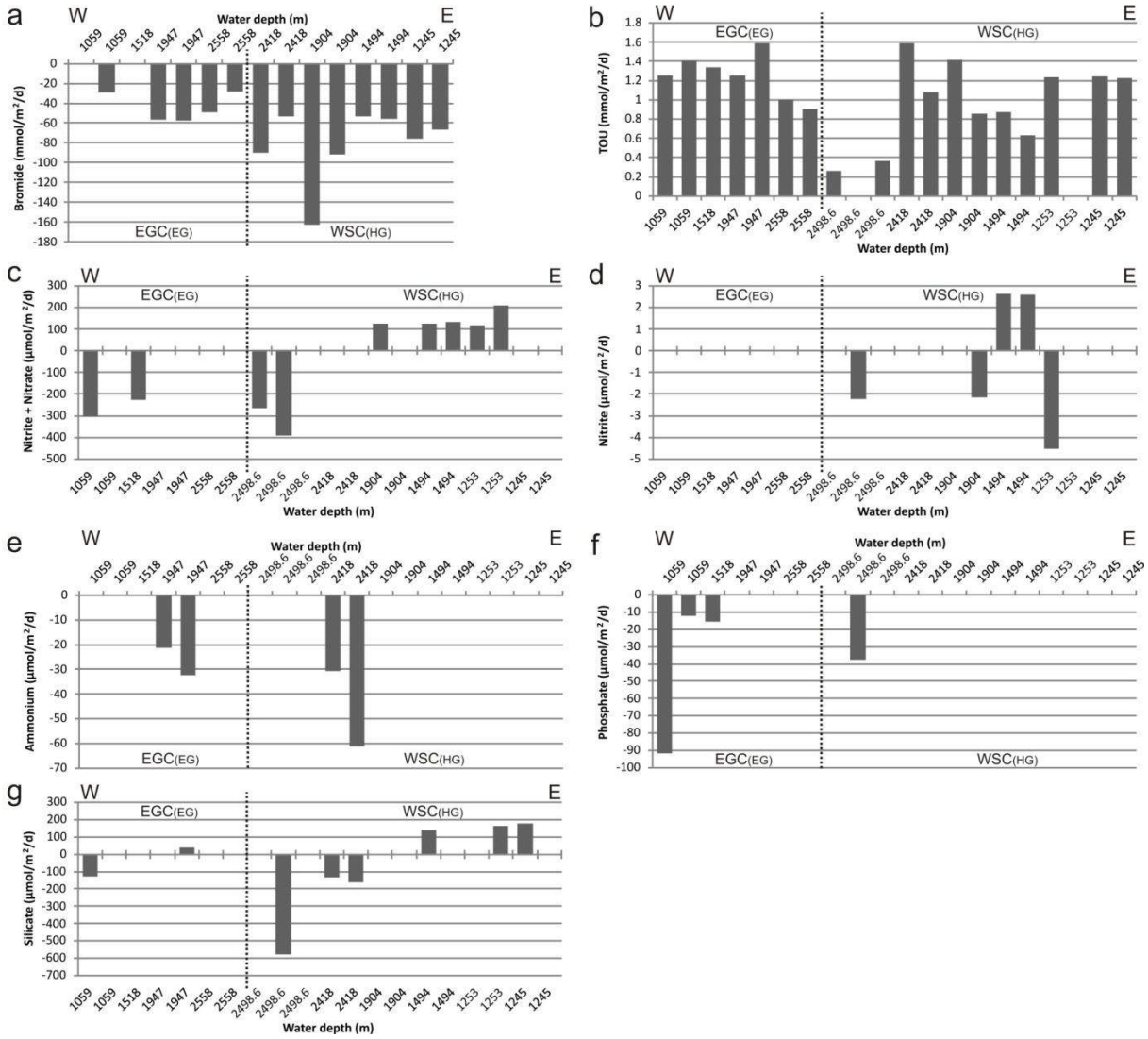

Fig. 3: (a) Bromide flux, (b) Total Oxygen Utilization (TOU) and (c-g) nutrient fluxes along the depth gradient, with separation according to site (EG-HG). Nutrient fluxes: (c) nitrite + nitrate (NO_2^- + NO_3^-); (d) nitrite (NO_2^-); (e) ammonium (NH_4^+); (f) phosphate (PO_4^{3-}); and (g) silicate (SiO_2).